genetic analyses, with results indicating that CPV (strain GRI) is closely related to VV and that the genetic distances from VAR were lowest for camelpox virus (<0.0155), next lowest for VV (<0.0259), high for MPV (<0.0307), and highest for ectromelia virus (<0.0354) (22). These analyses may lead to the prediction that complete genome sequence data from VVs or OPVs will provide insight into the efficacy of smallpox vaccine strains.

Therefore, we determined the complete genome sequences of the licensed m8, parental mO, and grandparental LO strains. Our data may be interpreted to mean that the LO-related vaccines have similar abilities that would induce immune protection, supporting the above-mentioned prediction. Only four missense mutations occurred among the >280 deduced ORFs of m8 during evolution from the parental mO strain. The major change was a truncating mutation of the B5R gene. It is therefore noted that B5R was the only destroyed gene in m8 compared to mO. Furthermore, m8 and mO possessed almost all ORFs corresponding to the vaccinia virus CPN strain (21). As the grandparental LO strain has never been plaque cloned, its genome sequence exhibited huge polymorphisms, which were previously suggested by analyses of restriction enzyme fragments and pock or plaque size (46, 52, 53). However, our PCR sequencing of the EEV *env*-related genes indicated that they were all preserved in mO, and in LO as well, and that m8 was probably derived from a low-virulence clone of divergent LO. This genomic background of m8 suggests that it functions like LO as a smallpox vaccine, except for B5R.

B5R is the only NAb-inducing antigen of EEV so far identified (19). EEVs are extracellular free virions released from infected cells and seem to be prevented by NAbs (12, 19, 44). Destruction of B5R reduced the formation of EEV 5- to 10-fold (36, 44, 54), although they comprise less than 1% of the total virus population (41). In light of these findings, a concern has arisen that the m8 vaccine seems to contain reduced amounts of EEV that lacks the B5R antigen and might not be protective against long-range spread of VAR EEV (5, 44, 45). Our study of multiple immunizations with recombinant B5R proteins adsorbed to adjuvant showed that antigenic activity was absent in the truncated B5R protein of m8 but present in the intact protein of LO. In addition, infection or vaccination with live VV induced very few anti-EEV NAbs, and repeated inoculations were required to induce moderate NAb levels (19, 44), probably because of the small EEV population. Alternatively, low levels of the antibodies may be due to the low sensitivity of conventional assay systems. Wyatt et al. recently reported that NAbs can be produced after a single percutaneous vaccination (56). They recently developed and used a highly sensitive system, a semiautomated flow cytometric assay with recombinant VV expressing enhanced green fluorescent protein (8).

It was therefore important to examine the levels of protection against virulent WR infection in m8-vaccinated mice, irrespective of the absence of EEV B5R-specific antibody responses. Our results confirmed that a single vaccination with m8, mO, and LO failed to induce detectable levels of anti-EEV and anti-B5R antibodies. Nevertheless, mice immunized with these vaccines were 100% protected against pathogenic WR challenge as early as 3 weeks after vaccination. Moreover, m8 with the whole B5R gene deleted protected mice from lethal WR challenge (32). These findings suggest that many viral antigens other than B5R are also involved in protective immunity to EEV. In this regard, antibodies to the A33R Env antigen did not neutralize EEV but provided mice with 100% protection (19). Anti-A33R might disrupt fragile EEV Env and convert to IMV, which is easily neutralized by anti-vaccinia antibodies (19, 28). Alternatively, A33R-specific cellular immunity may be crucial for protective immunity.

We have only limited knowledge about the protective immune mechanisms against smallpox. Experience with worldwide vaccination, however, has suggested that the protective mechanisms involve innate immunity, including interferons, natural killer cells, and complements, and also acquired immunity, including specific antibody- and T-cell-mediated immune responses (12). Indeed, recent papers have revealed the involvement of gamma interferon-expressing CD8 and CD4 T cells, vaccinia-specific cytotoxic T cells, and T-helper type 1 memory in humans (6, 7, 31, 48) and mice (16, 35, 49). Several studies conducted out of urgency in the last few years using smallpox vaccine candidates came to similar conclusions with regard to the contribution of overall immunity to smallpox protection (2, 9, 50, 56). Moreover, priming effects in vaccinated persons were recently shown to be long-lived or long-lasting, for as long as 75 years after vaccination (23). These historical and most recent studies imply that vaccine priming for immunological memory is important so that effecter components, such as NAbs, $CD4^+$ or $CD8^+$ T cells, and various cytokines can promptly be induced or boosted to protective levels by VAR infection, regardless of whether they are above measurable levels before infection. In support of this hypothesis, we found that mice that received a single dose of LO-related vaccines could not fully develop antibody responses as early as 3 weeks after vaccination but could produce enhanced levels of antibodies and complete immune protection after pathogenic-virus infection.

The need to produce safer and more effective vaccines may increase in the future. Here, we determined the nucleotide sequences of the whole genomes from the m8, intermediate mO, and original LO vaccine strains. The accumulating information on complete genome sequences of attenuated or pathogenic VVs and other OPVs will provide a basis for producing new genetically engineered vaccines. The double-stranded DNA genomes of OPVs are known to be highly stable. However, a single nucleotide insertion just upstream of the m8 B5R mutation site has recently been reported to restore the ORF to the parental mO phenotype after repeated (10 or more) virus passages. Although the repaired viruses were a marginal population, attenuation that is achieved by a deletion of the whole B5R gene prevented the reversion of m8- to mO-type viruses (32), which have, however, much lower virulence than LO and NYBH (24, 25, 39). In turn, the genetic manipulation of m8 to replace genes related to protective immunity, but not to pathogenicity, with the counterpart genes of VAR may make m8 more efficacious. It will be necessary to study in detail the correlation between individual gene functions and antigenicity of the gene products for inducing protective immunity in the future.

ACKNOWLEDGMENTS

We thank S. Hashizume for smallpox vaccine strains of vaccinia virus, LC16m8, LC16mO, and Lister Original (Elstree); Y. Sato for technical assistance; and N. Fujita, A. Kikuchi, M. Kudo, Y. Kuroda, S. Mimaki, M. Ohsawa, N. Okada, R. Sasaki, and S. Shinohara for assistance in sequencing and data processing.

This work was supported in part by grants from the Ministry of Health, Labor, and Welfare.

REFERENCES

1. **Appleyard, G., A. J. Hapel, and E. A. Boulter.** 1971. An antigenic difference between intracellular and extracellular rabbitpox virus. J. Gen. Virol. **13**:9–17.
2. **Belyakov, I. M., P. Earl, A. Dzutsev, V. A. Kuznetsov, M. Lemon, L. S. Wyatt, J. T. Snyder, J. D. Ahlers, G. Franchini, B. Moss, and J. A. Berzofsky.** 2003. Shared modes of protection against poxvirus infection by attenuated and conventional smallpox vaccine viruses. Proc. Natl. Acad. Sci. USA **100**:9458–9463.
3. **Birmingham, K., and G. Kenyon.** 2001. Smallpox vaccine development quickened. Nat. Med. **7**:1167.
4. **Chen, R. T., and J. M. Lane.** 2003. Myocarditis: the unexpected return of smallpox vaccine adverse events. Lancet **362**:1345–1346.
5. **Cohen, J.** 2002. Looking for vaccines that pack a wallop without the side effects. Science **298**:2314.
6. **Combadiere, B., A. Boissonnas, G. Carcelain, E. Lefranc, A. Samri, F. Bricaire, P. Debre, and B. Autran.** 2004. Distinct time effects of vaccination on long-term proliferative and IFN-producing T cell memory to smallpox in humans. J. Exp. Med. **199**:1585–1593.
7. **Drexler, I., C. Staib, W. Kastenmüller, S. Stevanovi, B. Schmidt, F. A. Lemonnier, H.-G. Rammensee, D. H. Busch, H. Bernhard, V. Erfle, and G. Sutter.** 2003. Identification of vaccinia virus epitope-specific HLA-A*0201-restricted T cells and comparative analysis of smallpox vaccines. Proc. Natl. Acad. Sci. USA **100**:217–222.
8. **Earl, P. L., J. L. Americo, and B. Moss.** 2003. Development and use of a vaccinia virus neutralization assay based on flow cytometric detection of green fluorescent protein. J. Virol. **77**:10684–10688.
9. **Earl, P. L., J. L. Americo, L. S. Wyatt, L. A. Eller, J. C. Whitbeck, G. H. Cohen, R. J. Eisenberg, C. J. Hartmann, D. L. Jackson, D. A. Kulesh, M. J. Martinez, D. M. Miller, E. M. Mucker, J. D. Shamblin, S. H. Zwiers, J. W. Huggins, P. B. Jahrling, and B. Moss.** 2004. Immunogenicity of a highly attenuated MVA smallpox vaccine and protection against monkeypox. Nature **428**:182–185.
10. **Enserink, M.** 2002. How devastating would a smallpox attack really be? Science **296**:1592–1595.
11. **Enserink, M.** 2004. Smallpox vaccines: looking beyond the next generation. Science **304**:809.
12. **Esposito, J. J., and F. Fenner.** 2001. Poxviruses, p. 2885–2921. *In* D. M. Knipe and P. M. Howley (ed.), Fields virology, 4th ed., vol. 2. Lippincott Williams & Wilkins, Philadelphia, Pa.
13. **Ewing, B., L. Hillier, M. C. Wendl, and P. Green.** 1998. Base-calling of automated sequencer traces using phred. I. Accuracy assessment. Genome Res. **8**:175–185.
14. **Ewing, B., and P. Green.** 1998. Base-calling of automated sequencer traces using phred. II. Error probabilities. Genome Res. **8**:186–194.
15. **Ferguson, N. M., M. J. Keeling, W. J. Edmunds, R. Gani, B. T. Grenfell, R. M. Anderson, and S. Leach.** 2003. Planning for smallpox outbreaks. Nature **425**:681–685.
16. **Fogg, C., S. Lustig, J. C. Whitbeck, R. J. Eisenberg, G. H. Cohen, and B. Moss.** 2004. Protective immunity to vaccinia virus induced by vaccination with multiple recombinant outer membrane proteins of intracellular and extracellular virions. J. Virol. **78**:10230–10237.
17. **Fulginiti, V. A., A. Papier, J. M. Lane, J. M. Neff, and D. A. Henderson.** 2003. Smallpox vaccination: a review, part II. Adverse events. Clin. Infect. Dis. **37**:251–271.
18. **Funahashi, S., T. Sato, and H. Shida.** 1988. Cloning and characterization of the gene encoding the major protein of the A-type inclusion body of cowpox virus. J. Gen. Virol. **69**:35–47.
19. **Galmiche, M. C., J. Goenaga, R. Wittek, and L. Rindisbacher.** 1999. Neutralizing and protective antibodies directed against vaccinia virus envelope antigens. Virology **254**:71–80.
20. **Gani, R., and S. Leach.** 2001. Transmission potential of smallpox in contemporary populations. Nature **414**:748–751.
21. **Goebel, S. J., G. P. Johnson, M. E. Perkus, S. W. Davis, J. P. Winslow, and E. Paoletti.** 1990. The complete DNA sequence of vaccinia virus. Virology **179**:247–266.
22. **Gubser, C., S. Hue, P. Kellam, and G. L. Smith.** 2004. Poxvirus genomes: a phylogenetic analysis. J. Gen. Virol. **85**:105–117.
23. **Hammarlund, E., M. W. Lewis, S. G. Hansen, L. I. Strelow, J. A. Nelson, G. J. Sexton, J. M. Hanifin, and M. K. Slifka.** 2003. Duration of antiviral immunity after smallpox vaccination. Nat. Med. **9**:1131–1137.
24. **Hashizume, S., H. Yoshizawa, M. Morita, and K. Suzuki.** 1985. Properties of attenuated mutant of vaccinia virus, LC16m8, derived from Lister strain, p. 421–428. *In* G. V. Quinnan (ed.), Vaccinia viruses as vectors for vaccine antigens. Elsevier Science Publishing Co., Amsterdam, The Netherlands.
25. **Hashizume, S., M. Morita, H. Yoshizawa, S. Suzuki, M. Arita, T. Komatsu, H. Amano, and I. Tagaya.** 1973. Internal symposium on smallpox vaccines, Bilthoven. Symp. Ser. Immunobiol. Stand. **19**:325–331.
26. **Henderson, D. A.** 1999. The looming threat of bioterrorism. Science **283**:1279–1282.
27. **Henderson, D. A., and B. Moss.** 1999. Smallpox and vaccinia, p. 74–97. *In* S. A. Plotkin and W. A. Orenstein (ed.), Vaccines. Saunders, Philadelphia, Pa.
28. **Ichihashi, Y.** 1996. Extracellular enveloped vaccinia virus escapes neutralization. Virology **217**:478–485.
29. **Joklik, W. K.** 1962. The purification of four strains of poxvirus. Virology **18**:9–18.
30. **Kaplan, E. H., D. L. Craft, and L. M. Wein.** 2002. Emergency response to a smallpox attack: the case for mass vaccination. Proc. Natl. Acad. Sci. USA **99**:10935–10940.
31. **Kennedy, J. S., S. E. Frey, L. Yan, A. L. Rothman, J. Cruz, F. K. Newman, L. Orphin, R. B. Belshe, and F. A. Ennis.** 2004. Induction of human T cell mediated immune responses after primary and secondary smallpox vaccination. J. Infect. Dis. **190**:1286–1294.
32. **Kidokoro, M., M. Tashiro, and H. Shida.** 2005. Genetically stable and fully effective smallpox vaccine strain constructed from highly attenuated vaccinia LC16m8. Proc. Natl. Acad. Sci. USA **102**:4152–4157.
33. **Kitts, P. A., M. D. Ayres, and R. D. Possee.** 1990. Linearization of baculovirus DNA enhances the recovery of recombinant virus expression vectors. Nucleic Acids Res. **18**:5667–5672.
34. **Lane, J. M., F. L. Ruben, J. M. Neff, and J. D. Millar.** 1969. Complications of smallpox vaccination, 1968. National surveillance in the United States. N. Engl. J. Med. **281**:1201–1208.
35. **Legrand, F. A., P. H. Verardi, K. S. Chan, Y. Peng, L. A. Jones, and T. D. Yilma.** 2005. Vaccinia viruses with a serpin gene deletion and expressing IFN-γ induce potent immune responses without detectable replication in vivo. Proc. Natl. Acad. Sci. USA **102**:2940–2945.
36. **Martinez-Pomares, L., R. J. Stern, and R. W. Moyer.** 1993. The ps/hr gene (B5R open reading frame homolog) of rabbitpox virus controls pock color, is a component of extracellular enveloped virus, and is secreted into the medium. J. Virol. **67**:5450–5462.
37. **Meltzer, M. I., I. Damon, J. W. LeDuc, and J. D. Millar.** 2001. Modeling potential responses to smallpox as a bioterrorist weapon. Emerg. Infect. Dis. **7**:959–969.
38. **Morita, M., K. Suzuki, A. Yasuda, A. Kojima, M. Sugimoto, K. Watanabe, H. Kobayashi, K. Kajima, and S. Hashizume.** 1987. Recombinant vaccinia virus LC16m0 or LC16m8 that expresses hepatitis B surface antigen while preserving the attenuation of the parental virus strain. Vaccine **5**:65–70.
39. **Morita, M., Y. Aoyama, M. Arita, H. Amano, H. Yoshizawa, S. Hashizume, T. Komatsu, and I. Tagaya.** 1977. Comparative studies of several vaccinia virus strains by intrathalamic inoculation into cynomolgus monkeys. Arch. Virol. **53**:197–208.
40. **O'Toole, T., M. Mair, and T. V. Inglesby.** 2002. Shining light on "Dark Winter." Clin. Infect. Dis. **34**:972–983.
41. **Payne, L. G.** 1980. Significance of extracellular enveloped virus in the in vitro and in vivo dissemination of vaccinia. J. Gen. Virol. **50**:89–100.
42. **Rice, C. M., C. A. Franke, J. H. Strauss, and D. E. Hruby.** 1985. Expression of Sindbis virus structural proteins via recombinant vaccinia virus: synthesis, processing, and incorporation into mature Sindbis virions. J. Virol. **56**:227–239.
43. **Rosenthal, S. R., M. Merchlinsky, C. Kleppinger, and K. L. Goldenthal.** 2001. Developing new smallpox vaccines. Emerg. Infect. Dis. **7**:920–926.
44. **Smith, G. L., A. Vanderplasschen, and M. Law.** 2002. The formation and function of extracellular enveloped vaccinia virus. J. Gen. Virol. **83**:2915–2931.
45. **Smith, G. L., and G. McFadden.** 2002. Smallpox: anything to declare? Nat. Rev. Immunol. **2**:521–527.
46. **Takahashi-Nishimaki, F., K. Suzuki, M. Morita, T. Maruyama, K. Miki, S. Hashizume, and M. Sugimoto.** 1987. Genetic analysis of vaccinia virus Lister strain and its attenuated mutant LC16m8: production of intermediate variants by homologous recombination. J. Gen. Virol. **68**:2705–2710.
47. **Takahashi-Nishimaki, F., S. Funahashi, K. Miki, S. Hashizume, and M. Sugimoto.** 1991. Regulation of plaque size and host range by a vaccinia virus gene related to complement system proteins. Virology **181**:158–164.
48. **Terajima, M., J. Cruz, G. Raines, E. D. Kilpatrick, J. S. Kennedy, A. L. Rothman, and F. A. Ennis.** 2003. Quantitation of CD8+ T cell responses to newly identified HLA-A*0201-restricted T cell epitopes conserved among vaccinia and variola (smallpox) viruses. J. Exp. Med. **197**:927–932.
49. **Tscharke, D. C., G. Karupiah, J. Zhou, T. Palmore, K. R. Irvine, S. M. M. Haeryfar, S. Williams, J. Sidney, A. Sette, J. R. Bennink, and J. W. Yewdell.** 2005. Identification of poxvirus CD8+ T cell determinants to enable rational design and characterization of smallpox vaccines. J. Exp. Med. **201**:95–104.
50. **Weltzin, R., J. Liu, K. V. Pugachev, G. A. Myers, B. Coughlin, P. S. Blum, R.**

Nichols, C. Johnson, J. Cruz, J. S. Kennedy, F. A. Ennis, and T. P. Monath. 2003. Clonal vaccinia virus grown in cell culture as a new smallpox vaccine. Nat. Med. **9**:1125–1130.

51. **Williamson, J. D., R. W. Reith, L. J. Jeffrey, J. R. Arrand, and M. Mackett.** 1990. Biological characterization of recombinant vaccinia viruses in mice infected by the respiratory route. J. Gen. Virol. **71**:2761–2767.
52. **Wittek, R., A. Menna, D. Schümperli, S. Stoffel, H. K. Müller, and R. Wyler.** 1977. *Hin*dIII and *Sy*I restriction sites mapped on rabbit poxvirus and vaccinia virus DNA. J. Virol. **23**:669–678.
53. **Wittek, R., H. K. Müller, A. Menna, and R. Wyler.** 1978. Length heterogeneity in the DNA of vaccinia virus is eliminated on cloning the virus. FEBS Lett. **90**:41–46.
54. **Wolffe, E. J., S. N. Isaacs, and B. Moss.** 1993. Deletion of the vaccinia virus B5R gene encoding a 42-kilodalton membrane glycoprotein inhibits extracellular virus envelope formation and dissemination. J. Virol. **67**:4732–4741.
55. **World Health Organization.** 1980. The global eradication of smallpox. Final report of the Global Commission for the Certification of Smallpox Eradication. World Health Organization, Geneva, Switzerland.
56. **Wyatt, L. S., P. L. Earl, L. A. Eller, and B. Moss.** 2004. Highly attenuated smallpox vaccine protects mice with and without immune deficiencies against pathogenic vaccinia virus challenge. Proc. Natl. Acad. Sci. USA **101**:4590–4595.
57. **Yamaguchi, M., M. Kimura, and M. Hirayama.** 1975. Report of the National Smallpox Vaccination Research Committee: study of side effects, complications and their treatments. Clin. Virol. **3**:269–278. (In Japanese.)
58. **Yasuda, A., J. Kimura-Kuroda, M. Ogimoto, M. Miyamoto, T. Sata, C. Takamura, T. Kurata, A. Kojima, and K. Yasui.** 1990. Induction of protective immunity in animals vaccinated with recombinant vaccinia viruses that express PreM and E glycoprotein of Japanese encephalitis virus. J. Virol. **64**:2788–2795.

Protease-mediated enhancement of severe acute respiratory syndrome coronavirus infection

Shutoku Matsuyama*, Makoto Ujike*, Shigeru Morikawa†, Masato Tashiro*, and Fumihiro Taguchi*‡

Division of Respiratory Viral Diseases and SARS, *Department of Virology III, Special Pathogens Laboratory, †Department of Virology I, National Institute of Infectious Diseases, Murayama Branch, Gakuen 4-7-1, Musashi-Murayama, Tokyo 208-0011, Japan

Edited by Peter Palese, Mount Sinai School of Medicine, New York, NY, and approved July 19, 2005 (received for review April 19, 2005)

A unique coronavirus severe acute respiratory syndrome-coronavirus (SARS-CoV) was revealed to be a causative agent of a life-threatening SARS. Although this virus grows in a variety of tissues that express its receptor, the mechanism of the severe respiratory illness caused by this virus is not well understood. Here, we report a possible mechanism for the extensive damage seen in the major target organs for this disease. A recent study of the cell entry mechanism of SARS-CoV reveals that it takes an endosomal pathway. We found that proteases such as trypsin and thermolysin enabled SARS-CoV adsorbed onto the cell surface to enter cells directly from that site. This finding shows that SARS-CoV has the potential to take two distinct pathways for cell entry, depending on the presence of proteases in the environment. Moreover, the protease-mediated entry facilitated a 100- to 1,000-fold higher efficient infection than did the endosomal pathway used in the absence of proteases. These results suggest that the proteases produced in the lungs by inflammatory cells are responsible for high multiplication of SARS-CoV, which results in severe lung tissue damage. Likewise, elastase, a major protease produced in the lungs during inflammation, also enhanced SARS-CoV infection in cultured cells.

cell entry | protease | spike protein | SARS

Severe acute respiratory syndrome (SARS) is caused by a SARS-associated coronavirus (SARS-CoV), a newly emergent member in a family of Coronaviridae (1–6). Unlike other human coronaviruses, SARS-CoV causes a fatal respiratory disease in humans (1–6). Coronavirus is an enveloped virus with a positive-stranded large genomic RNA with ≈30 kb (7). Spikes exist on the virion surface and resemble solar corona, each of which is composed of a trimer of the spike (S) protein (7, 8). The S protein is a type I fusion protein of an approximate molecular weight of 180 kDa. The prototypical coronavirus mouse hepatitis virus enters into cells via the cell surface, although a variant isolated from persistent infection enters from an endosome, the low pH of which induces its fusion activity (9). However, the entry pathway of SARS-CoV appears to be distinct from that of the other coronaviruses. Simmons *et al.* (10) hypothesized that SARS-CoV enters cells by an endosomal pathway, and S protein is activated for fusion by trypsin-like protease in an acidic environment. This idea is based on the following two findings: (*i*) SARS-CoV infection can be blocked by lysosomotropic agents, and (*ii*) S protein expressed on cells is activated for fusion by trypsin. These results were obtained by studies using pseudotype retroviruses harboring SARS-CoV S protein on the envelope and those using S protein expressed on cells by expression vectors (10).

In the present study, we show that various proteases, as well as trypsin, are effective in inducing the fusion of SARS-CoV-infected VeroE6 cells. These proteases facilitated SARS-CoV entry from the cell surface, which indicates that SARS-CoV has the potential to enter cells via two different pathways, either an endosomal or a nonendosomal pathway, depending on the presence of proteases. More interestingly, SARS-CoV entry from cell surface mediated by protease resulted in >100-fold more efficient infection than entry through endosome. Elastase, a major protease produced during lung inflammation, also manifested this enhancing effect. These findings suggest that severe illness in the lungs and intestines is attributable to the proteases produced in these organs during an inflammatory response or in the presence of certain physiological conditions.

Materials and Methods

Cells and Viruses. VeroE6 cells were grown in DMEM (Nissui, Tokyo), supplemented with 5% FBS (GIBCO/BRL). The SARS-CoV Frankfurt 1 strain, kindly provided by J. Ziebuhr (University of Würzburg, Würzburg, Germany) (1), was propagated and assayed by using Vero E6 cells.

Proteases. Various proteases were dissolved in PBS (pH 7.2) and used at the indicated concentrations in DMEM containing 5% FCS. The proteases used in this study were trypsin (Sigma, T-8802), thermolysin (Sigma, P 1512), chymotrypsin (Sigma, C-3142), dispase (Roche, 1 276 921), papain (Worthington, 53J6521), proteinase K (Wako, Tokyo), collagenase (Sigma, C-5183), and elastase (Sigma, E-0258).

Plaque Assay. VeroE6 cells prepared in 24-well plates were inoculated with 50 μl of 10-fold serially diluted virus samples and incubated at 37°C for 1 h. Cells were then cultured with 0.5 ml per well of DMEM containing 1% FCS and 0.75% methyl cellulose (Sigma) for 2 d. Cells were fixed with 1 ml of 10% formaldehyde per well for at least 2 h. After removing the culture fluids, cells were irradiated overnight under a UV lamp and stained with crystal violet. Plaques produced by SARS-CoV were counted under light microscopy. Titration was done in duplicate and infectivity was displayed by plaque-forming units (pfu).

Western Blotting. S protein expressed in Vero E6 cells was analyzed by Western blotting. Preparation of cell lysates, SDS/PAGE, and electrical transfer of the protein onto a transfer membrane were described (11). S protein was detected with anti-S Ab, IMG-557 (Imgenex, San Diego) and horseradish peroxidase-conjugated anti-rabbit IgG Ab (anti-R-IgG, ALI3404, BioSource International, Camarillo, CA). The bands were visualized by using enhanced chemiluminescence reagents (ECL-plus, Amersham Pharmacia) on a LAS-1000 instrument (Fuji).

Real-Time PCR. VeroE6 cells in 96-well culture plates were treated with DMEM containing 1 μM bafilomycin (Baf; Sigma, B-1793) and 5% FCS (DMEM plus Baf) at 37°C for 30 min and then chilled on ice for 10 min. Approximately 10^4 pfu of virus in DMEM plus Baf were infected to 10^4 cells on ice; multiplicity of

This paper was submitted directly (Track II) to the PNAS office.

Abbreviations: SARS-CoV, severe acute respiratory syndrome-coronavirus; S, spike; pfu, plaque-forming unit; moi, multiplicity of infection; Baf, bafilomycin.

‡To whom correspondence should be addressed. E-mail: ftaguchi@nih.go.jp.

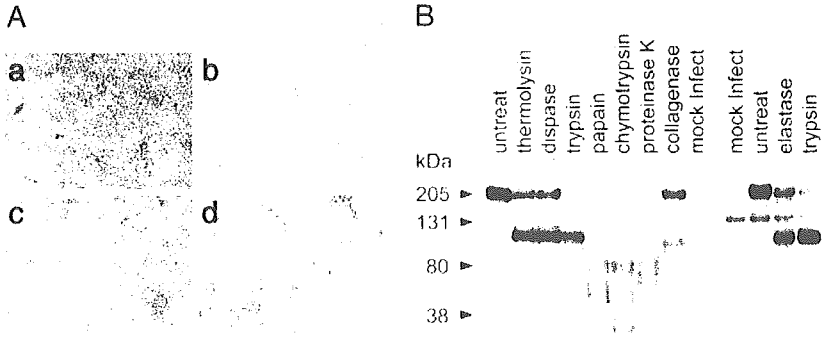

Fig. 1. Induction of cell-fusion and SARS-CoV S protein cleavage by proteases. (*A*) Syncytium formation after treatment with trypsin. VeroE6 cells cultured in 24-well plates were infected (*b* and *d*) or mock-infected (*a* and *c*) with the SARS-CoV Frankfurt 1 strain at moi = 0.5 and incubated at 37°C for 20 h. Cells were washed once with PBS and treated (*c* and *d*) or untreated (*a* and *b*) with 200 μg/ml trypsin for 5 min. Those cells were cultured for a further 4 h and observed by microscopy. (*B*) Western blot analysis of S protein treated with various proteases. Cells infected as described above were treated either with thermolysin (200 μg/ml), dispase (1 unit/ml), trypsin (200 μg/ml), papain (0.74 unit/ml), chymotrypsin (1 mg/ml), proteinase K (8 μg/ml) collagenase (200 μg/ml), or elastase (1 mg/ml), as described above. Soon after treatment, cells were lysed with lysing buffer, and S protein was analyzed by Western blot after SDS/PAGE. To detect the S protein (S2 fragment), mAb IMG-557 was used at a concentration of 5 μg/ml.

infection (moi) was at 1. After 30-min adsorption, the virus was removed, and infected cells were treated for 5 min with various concentrations of proteases in DMEM plus Baf that was prewarmed at room temperature. After protease was removed, cells were cultured in DMEM plus Baf at 37°C for 6 h. Vero E6 cell monolayers in 24-well plates were infected with 10 pfu of SARS-CoV (moi = 0.0001). After 30-min adsorption, cells were cultured in DMEM containing 5% FCS in the presence or in the absence of various proteases for 20 h. To isolate cellular RNA, 100 and 500 μl of isogen (Nippon Gene, Toyama, Japan) were added to each well of 96- and 24-well plates, respectively, together with 5 μg of yeast RNA as a carrier for 2-propanol precipitation. RNA was prepared according to the manufacturer's instructions and finally dissolved in 20 μl of diethyl pyrocarbonate-treated water. Real-time PCR was performed to estimate the amounts of mRNA9 in a final volume of 20 μl of 1× LightCycler RNA Master Mix (Roche Diagnostics) by using the RNA isolated as described above. For amplification of the fragment from mRNA9, we used 500 nM of a pair of oligonucleotides 5′-CTCGATCTCTTGTAGATCTG-3′ (SARS leader) and 5′-TCTAAGTTCCTCCTTGCCAT-3′ (SARS mRNA9 reverse). Amplified DNA from mRNA has 240 bases. With these primers, genomic RNA was not detected because the fragment to be amplified from genomic RNA would be ≈30 kb. For detection by hybridization, 200 nM each of the hybridization probes 5′-ACCAGAATGGAGGACGCAATGGGGCAAG-3′ (3′FITC labeled), 5′-CCAAAACAGCGCCGACCCCAAGGTTTAC-3′ (5′LCRed640 labeled) were used. PCR analysis was performed under the following conditions [reverse transcription: 61°C, 20 min; PCR, 95°C, 30 s (95°C, 5 s; 55°C, 15 s; 72°C, 10 s) ×45 cycles] with a LightCycler instrument (Roche Diagnostics). To measure the amounts of viruses that entered into cells, we infected cells with 10-fold stepwise diluted SARS-CoV from 10^6 to 10^2 pfu, and the amounts of mRNA9 were determined by real-time PCR. The amounts of virus that entered into cells after protease treatment were calculated from a calibration line obtained as above and shown as relative mRNA levels. When relative mRNA9 was higher than 10^6 pfu, samples were diluted and reexamined so that they were placed between 10^6 and 10^2 pfu.

Results

Activation of Cell Fusion and SARS-CoV S Protein Cleavage by Various Proteases. VeroE6 cells susceptible to SARS-CoV were infected with the Frankfurt-1 strain of SARS-CoV at a moi of 0.5, and those infected cells were treated with trypsin at 20 h after infection. Cell fusion was detected from 2 h after trypsin treatment (Fig. 1*Ad*). Fusion was also found after treatment with thermolysin or dispase (data not shown). Little or no fusion occurred after treatment with papain, chymotrypsin, proteinase K, or collagenase. S proteins in cells treated with proteases that induce fusion were cleaved approximately in the middle (Fig. 1*B*), a finding similar to that of Simmons *et al.* (10). In contrast, no apparent S2 band was detected in cells bearing S proteins treated with proteases that failed to induce fusion (Fig. 1*B*). These results showed that various proteases, including trypsin, activate the fusion activity of the SARS-CoV S protein by inducing its cleavage. Further, SARS-CoV infection was extensively inhibited by treatment of cells with Baf (Fig. 2*A*, no Baf vs. Baf without protease). These results suggest that SARS-CoV takes an endosomal pathway for its entry, and that S protein cleavage is important for fusogenicity, which is consistent with the conclusions of a previous report (10).

SARS-CoV Entry from Cell Surface Facilitated by Proteases. If the hypothesis proposed by Simmons *et al.* (10) is correct, we can make SARS-CoV enter cells directly from their surface by attaching the virus there and treating them with trypsin and other proteases that induce fusion. Treatment of VeroE6 cells with Baf at a concentration of 1 μM suppressed SARS-CoV infection via the endosomal pathway to $<1/100$, as shown in Fig. 2*A*. The cells treated with Baf were inoculated with SARS-CoV at a moi of 1 and incubated on ice for 30 min (adsorption on ice does not allow virus to enter cells). Then cells were treated with various proteases for 5 min at room temperature and incubated at 37°C for 6 h. Virus entry was estimated by the newly synthesized mRNA9 measured quantitatively by real-time PCR. A calibration curve of real-time PCR (Fig. 2*C*), showing the level of mRNA9 after infection with 10-fold diluted SARS-CoV, was used to estimate the amount of infected virus from the mRNA levels. As shown in Fig. 2*A*, thermolysin and trypsin, two proteases with fusion-inducing activity, extensively facilitated viral entry. In contrast, two proteases that did not induce fusion, papain and collagenase failed to do so. Treatment of cells with trypsin before virus infection did not facilitate viral entry (Fig. 2*B*), indicating that effects of trypsin on cells are not involved in this infection. Other proteases did not influence the SARS-CoV infection as trypsin, when treated before virus inoculation (data not shown). Protease treatment of SARS-CoV before infection did not enhance infectivity but reduced it by 10- to 100-fold (data

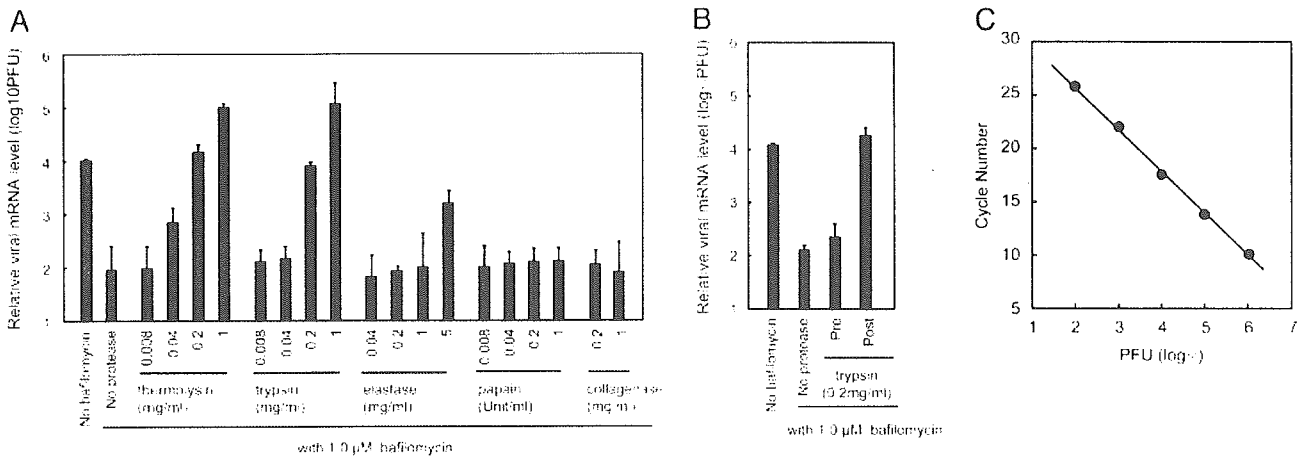

Fig. 2. Entry of SARS-CoV from cell surface facilitated by proteases. (*A*) Effect of proteases on SARS-CoV entry into VeroE6 cells treated with Baf. VeroE6 cells in 96-well plates were treated with Baf at a concentration of 1 μM at 37°C for 30 min, placed on ice and infected with SARS-CoV at moi = 1 for 30 min. Then, cells were treated with various concentrations of different proteases at room temperature for 5 min and cultured in the presence of Baf for a further 6 h. The amount of mRNA9 was measured quantitatively by real-time PCR. Cells untreated with Baf or those treated with Baf but untreated with protease were used as controls. The relative viral mRNA level is displayed by virus infectivity (pfu) calculated from a calibration line shown in *C*. (*B*) Cells treated with Baf at 37°C for 30 min were then treated with trypsin at room temperature for 5 min before (pre) or after (post) virus inoculation, and virus infection was estimated quantitatively by real-time PCR as described above. (*C*) Calibration in real-time PCR. VeroE6 cells in 94-well plates were infected with 10-fold step diluted viruses, and mRNA9 levels at 6 h after infection were estimated by real-time PCR. The relationship is shown between inoculated pfu (*x* axis) and cycles of real-time PCR to reach a positive level (amount of mRNA9) (*y* axis).

not shown). We believe these results demonstrate that SARS-CoV, when adsorbed onto the cell surface, fuse with the plasma membrane of its envelope with S protein, which is cleaved into S1 and S2 by proteases with fusion-inducing activity. This suggests a nonendosomal, direct entry of SARS-CoV into cells in the presence of proteases. Those findings also support the hypothesis drawn by Simmons *et al.* (10) that trypsin-like protease plays an important role in facilitating membrane fusion.

Enhancement of SARS-CoV Infection by Various Proteases. Treatment with a high concentration of thermolysin and trypsin augmented virus entry or replication by 10-fold or higher, as compared with the standard infection (Fig. 2*A*, e.g., compare bar 6 or bar 10 with bar 1 from the left). We then compared the replication kinetics of SARS-CoV in cells treated with Baf and a high concentration of trypsin with that of cells maintained without Baf or trypsin. The level of mRNA9 was always ≈10-fold higher in trypsin-treated cells at any given time during the early period of infection (Fig. 3). These data also imply that viral replication after entry via the cell surface proceeds ≈1 h ahead of that via the endosomal pathway, suggesting that the surface route is more efficient for rapid viral replication.

Because SARS-CoV replication was shown to be enhanced by trypsin treatment, we next assessed the efficiency of virus spread in the presence or absence of trypsin in a low moi, which mimics natural infection in target organs. Virus (10 pfu) were inoculated onto 10^5 confluent VeroE6 cells (moi = 0.0001), and the cells were incubated at 37°C for 20 h in the media with or without trypsin. The level of mRNA9 estimated quantitatively by real-time RT-PCR showed that virus replication was 100- to 1,000-fold higher when cells were cultured in the presence of trypsin, when compared with replication in the absence of trypsin (Fig. 4*A*). Viral infectivity of the supernatants in SARS-CoV-infected cells cultured with or without trypsin also indicated that trypsin treatment enhanced viral growth by ≈100-fold (Fig. 4*B*). We also examined growth kinetics of SARS-CoV in the presence of low-concentration proteases (62.5 μg/ml trypsin, 125 μg/ml elastase) that do not detach cells from plates during culture for 42 h. It was also shown that protease enhanced virus replication (Fig. 4*C*) with remarkable fusion formation (Fig. 4*D*). All of these results strongly suggest that the virus spreads efficiently from cell to cell in the presence of trypsin, which cleaves S to S1 and S2 to allow cell entry of SARS-CoV via the cell surface.

We next examined the effects on low moi by other proteases that facilitate SARS-CoV entry from VeroE6 cell surface. As shown in Fig. 5, all of the proteases that produce S2 (Fig. 1*B*) and that induce cell-cell fusion enhanced virus spread. In contrast, those proteases that did not generate S2 and that did not induce cell-cell fusion failed to enhance the infection. These observations suggest that proteases that facilitate SARS-CoV entry from the cell surface support efficient SARS-CoV infection. Thus, protease is likely to be responsible for the high multiplication of

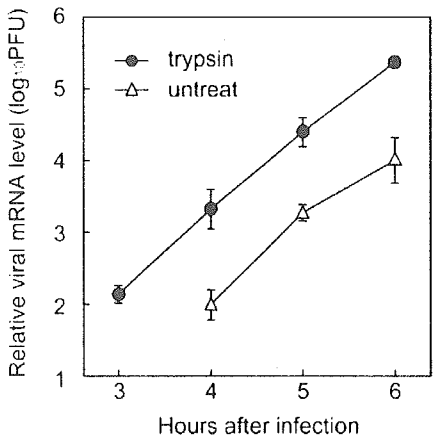

Fig. 3. Kinetics of mRNA9 synthesis after treatment of trypsin. VeroE6 cells were treated with Baf, infected with SARS-CoV, and treated with 200 μg/ml trypsin as described in the legend to Fig. 2*A*. The amount of mRNA9 synthesized was monitored by real-time PCR at 3–6 h after inoculation. VeroE6 cells without any treatment were also infected as a control (untreated). Relative viral mRNA level is displayed by virus infectivity (pfu) calculated from the calibration line shown in Fig. 2*C*.

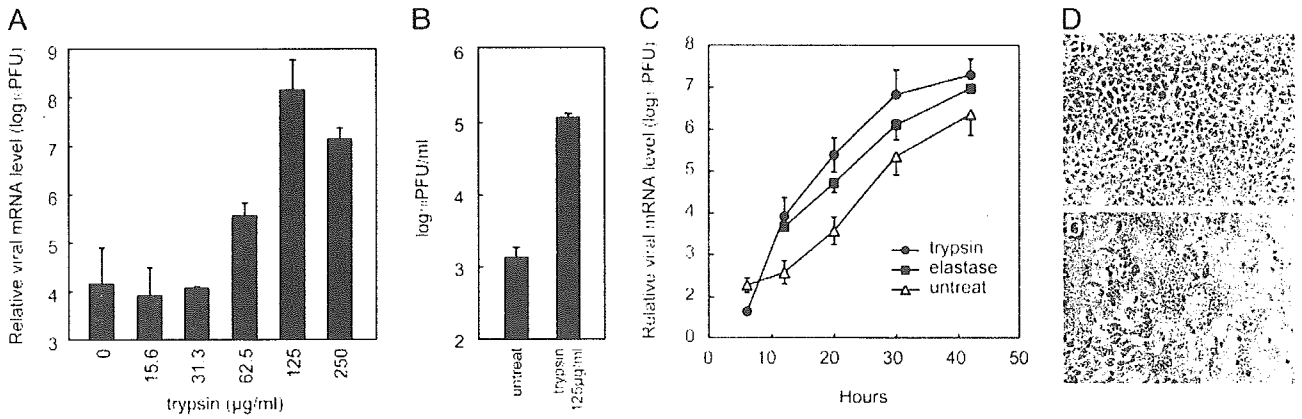

Fig. 4. Enhancement of SARS-CoV infection by proteases. (*A*) Effect of trypsin on virus replication in VeroE6 cells. Approximately 1×10^5 VeroE6 cells cultured in 24-well plates were infected with 10 pfu of SARS-CoV (moi = 0.0001) and cultured in the presence of varied trypsin concentrations. Viral replication was estimated at 20 h after infection by the amount of mRNA9, as measured by real-time PCR. (*B*) Viral infectivity was examined by plaque assay after 20-h incubation in the presence or absence of trypsin (125 μg/ml). (*C*) Viral growth kinetics after infection was examined in cultures in the presence or absence of trypsin (62.5 μg/ml) or elastase (125 μg/ml) by real-time PCR. Cells were harvested from 4 to 42 h after infection at intervals and the level of mRNA9 was monitored. Relative viral mRNA level is displayed by virus infectivity (pfu) calculated from a calibration line (*A–C*). (*D*) Cytopathic changes of virus-infected cells cultured in the presence (*b*) or absence (*a*) of trypsin (125 μg/ml) for 42 h are shown.

SARS-CoV in the major target organs of SARS, such as the lungs and bronchus, where various proteases are produced (e.g., by inflammatory cells), as well as in the intestines, where a number of proteases are physiologically secreted.

One of the major proteases produced by inflammatory cells in the lungs is an elastase produced by neutrophils (12), the accumulation of which was reported in the lungs of SARS patients (13). The level of elastase in bronchoalveolar lavage fluids was reported to reach levels as high as 700 μg/ml (12). Accordingly, we determined whether this protease has the potential to enhance SARS-CoV infection in a fashion similar to that of trypsin or thermolysin. Elastase was revealed to enhance SARS-CoV infection in cultured VeroE6 cells in terms of S protein cleavage (Fig. 1*B*), its cell-surface-mediated entry pathway (Fig. 2*A*), and its growth enhancement ability after low moi

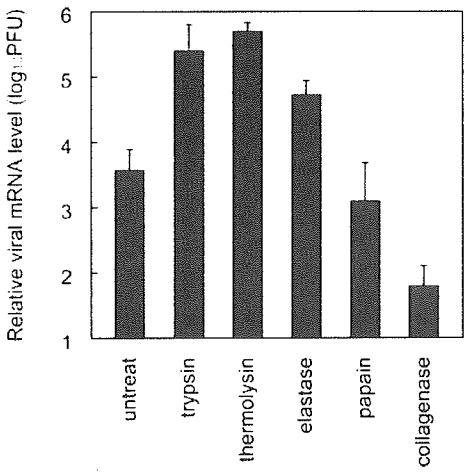

Fig. 5. Effect of various proteases on virus replication in VeroE6 cells. VeroE6 cells in 24-well plates were infected as described in Fig. 4 and cultured in the presence of trypsin (62.5 μg/ml), thermolysin (12.5 μg/ml), elastase (125 μg/ml), papain (0.037 unit/ml), or collagenase (200 μg/ml). At 20 h after infection, the amounts of mRNA9 were measured by real-time PCR. Relative viral mRNA level is displayed by virus infectivity (pfu) calculated from the calibration line.

(Figs. 4*C* and 5). These results strongly suggest that SARS-CoV replication can be enhanced in the lungs by elastase.

Discussion

The SARS-CoV gene and viral antigens were found in a number of organs, such as the liver, cerebrum, pancreas, and kidneys, as well as in such major target organs as the bronchus, lungs, and intestines (14–17), with the latter showing drastic tissue damage by SARS-CoV infection, whereas the other organs were not so severely affected. Although the pathogenic mechanism of SARS has not been elucidated, the present study suggests that proteases secreted in major target organs play an important role in the high multiplication of virus in those organs, which, in turn, results in severe tissue damage. An initial infection by SARS-CoV in pneumocytes via its receptor ACE2 (18), the endosomal pathway, could induce inflammation that generates a variety of proteases such as elastase. Once those proteases are present in the lungs, they may mediate an ensuing robust infection, which may result in enhanced replication of SARS-CoV in the lungs. Although lung damage is postulated to be mediated by cytokines by a so-called cytokine storm (14, 16), higher virus multiplication could also contribute to the cytokine storm by killing a large number of infected cells. A variety of proteases secreted in the small intestines, another major target organ of SARS-CoV, could also be responsible for the high growth of SARS-CoV in these tissues, which could result in a high rate of diarrhea in SARS patients (19, 20).

Protease-mediated enhancement of infection is known for orthomyxovirus and paramyxovirus infections (21–24), in which their envelope glycoprotein is not fully cleaved in *de novo* synthesized cells, and thus the virus particles produced contain partially cleaved or uncleaved glycoprotein. Those glycoproteins on virions are cleaved after treatment with protease, which results in the enhancement of infectivity. Thus, trypsin affects directly virons and increases the infectivity of those viruses. However, enhancement of SARS-CoV infection by trypsin or other proteases is mediated by another mechanism. Although trypsin treatment *in vitro* induces cleavage of the S protein on virions, such treatment never enhances SARS-CoV infectivity but reduces it to 1/10–1/100 of the original titer. Only S protein bound to its receptor ACE2 and cleaved by proteases could obtain fusion activity. Based on this idea, it is most likely that

binding of S protein to ACE2 induces conformational changes of the S, which is inevitable to be correctly processed for fusion activity by proteases. In other words, proteases can successfully induce the fusion activity of S protein only after S-ACE2 binding. Alternatively, protease treatment of virions digests out the S1 portion important for ACE2 binding, resulting in a loss of infectivity, whereas S2 alone is sufficient for fusion after binding to its receptor despite loss of the S1 fragment.

Why is the infection via the endosomal pathway not as efficient as direct infection from the cell surface? Throughout our examinations, replication deriving from the cell surface pathway began 1 h ahead of that via the endosomal pathway. We assume that a virus needs ≈1 h for trafficking from the cell surface where virion binds to ACE2 to the endosome. When cells are infected with an extremely low moi, a condition that occurs in natural infection, a 100- to 1,000-fold higher rate of infection was observed in the presence of proteases. Thus a 10-fold difference at 6 h after inoculation could result in a 1,000-fold difference, provided that one cycle of SARS-CoV replication is ≈6 h (25) and three rounds of infection take place within 20 h.

The present studies suggest that coinfection of SARS-CoV with some other non- or low-pathogenic respiratory agents, such as *Chlamydia*, mycoplasma, or bacteria, results in severe lung disease, which is attributed to the proteases produced by the infection with those non-SARS-CoV agents, as has been shown by the enhancement of respiratory diseases caused by influenza virus coinfected with nonpathogenic bacteria (26, 27). Studies are in progress to see whether coinfection exacerbates pneumonia in mice infected with SARS-CoV.

We thank Miyuki Kawase for excellent technical assistance throughout the experiments, John Ziebuhr (University of Würzburg, Würzburg, Germany) for providing SARS-CoV Frankfurt-1, and Judith White (University of Virginia, Charlottesville) for valuable comments on this work. We also thank the colleagues of our institute, especially Shuetsu Fukushi, Keiko Nakagaki, Kohji Ishii, and Yasuko Yokota, for valuable discussions and encouragement throughout the research. This work was supported by Ministry of Education, Culture, Sports, Science, and Technology Grant 16017308 and Ministry of Health, Labor, and Welfare Grant H16-Shinkoh-9.

1. Ksiazek, T. G., Erdman, D., Goldsmith, C., Zaki, S. R., Peret, T., Emery, S., Tong, S., Urbani, C., Comer, J. A., Lim, W., *et al.* (2003) *N. Engl. J. Med.* **348,** 1953–1966.
2. Drosten, C., Gunther, S., Preiser, W., Van Der Werf, S., Brodt, H. R., Becker, S., Rabenau, H., Panning, M., Kolesnikowa, L., Fouchier, R. A., *et al.* (2003) *N. Engl. J. Med.* **348,** 1967–1976.
3. Marra, M. A., Jones, S. J., Astell, C. R., Holt, R. A., Brooks-Wilson, A., Butterfield, Y. S., Khattra, J., Asano, J. K., Barber, S. A., Chan, S. Y., *et al.* (2003) *Science* **300,** 1399–1404.
4. Rota, P. A., Oberste, M. S., Monroe, S. S., Nix, W. A., Campagnoli, R., Icenogle, J. P., Penaranda, S., Bankamp, B., Maher, K., Chen, M. H., *et al.* (2003) *Science* **300,** 1394–1399.
5. The Chinese SARS Molecular Epidemiology Consortium (2004) *Science* **303,** 1666–1669.
6. Peiris, J. S., Guan, Y. & Yuen, K. Y. (2005) *Nat. Med.* **10,** 588–597.
7. Lai, M. M. C. & Cavanagh, D. (1997) *Adv. Virus Res.* **48,** 1–100.
8. Tyrell, D. A. J., Almeida, J. D., Berry, D. M., Cunningham, C. H., Hamre, D., Hofstad, M. S., Mallucci, L. & McIntosh, K. (1968) *Nature* **220,** 650.
9. Gallagher, T. M., Escarmis, C. & Buchmeier, M. J. (1991) *J. Virol.* **65,** 1916–1928.
10. Simmons, G., Reeves, J. D., Rennekamp, A. J., Amberg, S. M., Piefer, A. J. & Bates, P. (2004) *Proc. Natl. Acad. Sci. USA* **101,** 4240–4245.
11. Matsuyama, S. & Taguchi, F. (2000) *Virology* **273,** 80–89.
12. Kawabata, K., Haio, T. & Matsuoka, S. (2002) *Eur. J. Pharmacol.* **451,** 1–10.
13. Wong, C. K., Lam, C. W., Wu, A. K., Ip, W. K., Lee, N. L., Chan, I. H., Lit, L. C., Hui, D. S., Cha, M. H., Chung, S. S., *et al.* (2004) *Clin. Exp. Immunol.* **136,** 95–103.
14. Nicholls, J. M., Poon, L. L., Lee, K. C., Ng, W. F., Lai, S. T., Leung, C. Y., Chu, C. M., Hui, P. K., Mak, K. L., Lim, W., *et al.* (2003) *Lancet* **361,** 1773–1778.
15. Peiris, J. S. M., Lai, S. T., Poon, L. L. M., Guan, Y., Yam, L. Y. C., Lim, W., Nicholls, J., Yee, W. K. S., Yan, W. W., Cheung, M. T., *et al.* (2003) *Lancet* **361,** 1767–1772.
16. Tse, G. M., To, K. F., Chan, P. K., Lo, A. W., Ng, K. C., Wu, A., Lee, N., Wong, H. K., Mac, S. M., Chan, K. F., *et al.* (2004) *J. Clin. Pathol.* **57,** 260–265.
17. To, K. F. & Lo, A. W. (2004) *J. Pathol.* **203,** 740–743.
18. Li, W., Moore, M. H., Vasilieva, N., Sui, J., Wong, S. K., Berne, M. A., Somasundaran, M., Sullivan, J. L., Luzuriaga, K., Greenough, T. C., *et al.* (2003) *Nature* **426,** 450–454.
19. Zhan, J., Chen, W., Li, C., Wu, W., Li J., Jiang, S., Wang, J., Zeng, Z., Huang, Z. & Huang, H. (2003) *Clin. Med. J.* **116,** 1265–1266.
20. Leung, W. K., To, K. F., Chan, P. K., Chan, H. L., Wu, A. K., Lee, N., Yuen, K. Y. & Sung, J. J. (2003) *Gastroenterology* **125,** 1011–1017.
21. Rott, R., Orlich, M. & Blodorn, J. (1975) *Virology* **68,** 426–439.
22. Nagai, Y., Klenk, H. D. & Rott, R. (1976) *Virology* **72,** 494–508.
23. Ohuchi, M. & Homma, M. (1976) *J. Virol.* **18,** 1147–1150.
24. Tashiro, M., Yokogoshi, Y., Tomita, K., Seto, J. T., Rott, R. & Hido, H. (1992) *J. Virol.* **72,** 11–16.
25. Ng, M.-L., Tan, S.-H., See, E. E., Ooi, E. E. & Ling, A. E. (2003) *J. Gen. Virol.* **84,** 3291–3303.
26. Tashiro, M., Ciborowski, P., Klenk, H.-D., Pulverer, G. & Rott, R. (1987) *Nature (London)* **325,** 536–537.
27. Kishida, N., Sakoda, Y., Eto, M., Sunaga, Y. & Kida, H. (2004) *Arch. Virol.* **149,** 2095–2140.

Journal of General Virology (2005), 86, 2269–2274 DOI 10.1099/vir.0.80955-0

Short Communication

Vesicular stomatitis virus pseudotyped with severe acute respiratory syndrome coronavirus spike protein

Shuetsu Fukushi,[1] Tetsuya Mizutani,[1] Masayuki Saijo,[1] Shutoku Matsuyama,[2] Naoko Miyajima,[2] Fumihiro Taguchi,[2] Shigeyuki Itamura,[3] Ichiro Kurane[1] and Shigeru Morikawa[1]

Correspondence
Shuetsu Fukushi
fukushi@nih.go.jp

Special Pathogens Laboratory, Department of Virology I[1], Laboratory of Respiratory Viral Diseases and SARS[2] and Laboratory of Influenza Virus, Department of Virology III[3], National Institute of Infectious Diseases, Gakuen 4-7-1, Musashimurayama, Tokyo 208-0011, Japan

Severe acute respiratory syndrome coronavirus (SARS-CoV) contains a single spike (S) protein, which binds to its receptor, angiotensin-converting enzyme 2 (ACE2), induces membrane fusion and serves as a neutralizing antigen. A SARS-CoV-S protein-bearing vesicular stomatitis virus (VSV) pseudotype using the VSVΔG* system was generated. Partial deletion of the SARS-CoV-S protein cytoplasmic domain allowed efficient incorporation into VSV particles and led to the generation of a pseudotype (VSV-SARS-St19) at high titre. Green fluorescent protein expression was demonstrated as early as 7 h after infection of Vero E6 cells with VSV-SARS-St19. VSV-SARS-St19 was neutralized by anti-SARS-CoV antibody and soluble ACE2, and its infection was blocked by treatment of Vero E6 cells with anti-ACE2 antibody. These results indicated that VSV-SARS-St19 infection is mediated by SARS-CoV-S protein in an ACE2-dependent manner. VSV-SARS-St19 will be useful for analysing the function of SARS-CoV-S protein and for developing rapid methods of detecting neutralizing antibodies specific for SARS-CoV infection.

Received 9 February 2005
Accepted 21 April 2005

Severe acute respiratory syndrome (SARS) is a recently described infectious disease caused by a newly identified coronavirus, SARS-CoV (Drosten *et al.*, 2003; Ksiazek *et al.*, 2003). With a mortality rate of over 9%, SARS has had major health and socio-economic impacts (Fouchier *et al.*, 2003). Despite intensive efforts, no effective antiviral treatments against SARS have yet been established. Studies of SARS-CoV infection have been limited because of the highly infectious nature of the virus and the problem of recent cases in which infection was suspected to have occurred in research laboratories.

Entry of SARS-CoV into susceptible cells is mediated by binding of the viral spike (S) protein to receptor molecules. The SARS-CoV-S protein has a 13 aa signal peptide at its N terminus, a single ectodomain of 1182 aa and a transmembrane region followed by a cytoplasmic domain of 28 aa (Marra *et al.*, 2003; Rota *et al.*, 2003). Recently, pseudotyped retroviruses bearing SARS-CoV-S protein have been generated by several laboratories (Hofmann *et al.*, 2004; Nie *et al.*, 2004; Simmons *et al.*, 2004). It has been shown that these pseudotyped viruses have a cell tropism identical to SARS-CoV and that their infection is dependent on a receptor molecule, angiotensin-converting enzyme 2 (ACE2), indicating that infection is mediated solely by SARS-CoV-S protein. Pseudotyped viruses provide a safe viral entry model because of their inability to produce infectious progeny virus. A quantitative assay of pseudotyped virus infection could facilitate research on SARS-CoV entry, cell tropism and neutralizing antibodies. Interestingly, it was reported that a pseudotyped retrovirus bearing a SARS-CoV-S protein variant with a truncation in the cytoplasmic domain was incorporated more efficiently into retrovirus particles than the full-length S protein (Giroglou *et al.*, 2004; Moore *et al.*, 2004).

Another pseudotyping system with a vesicular stomatitis virus (VSV) particle [the VSVΔG* system, in which the VSV G gene is replaced by the green fluorescent protein (GFP) gene] was reported previously to produce pseudotype VSV particles incorporating the envelope glycoproteins of several RNA viruses (i.e. measles virus, hantavirus, Ebola virus or hepatitis C virus; Matsuura *et al.*, 2001; Ogino *et al.*, 2003; Takada *et al.*, 1997; Tatsuo *et al.*, 2000). This system may be useful for research on viral envelope glycoproteins due to the ability of the pseudotype to grow at high titres in a variety of cell lines. The pseudotype virus titre obtained with the VSVΔG* system is generally higher than that of the pseudotype retrovirus system (Ogino *et al.*, 2003). Furthermore, infection of target cells with pseudotype VSV can be readily detected as GFP-positive cells by 16 h

Detection of expression of SARS-CoV-S protein and soluble mutated ACE2 are available as supplementary material in JGV Online.

post-infection (p.i.) because of the high level of GFP expression in the VSVΔG* system (Ogino *et al.*, 2003). In contrast, the time required for infection in the pseudotype retrovirus system is 48 h (Moore *et al.*, 2004; Nie *et al.*, 2004), which is similar to the time required for SARS-CoV to replicate to a level that results in plaque-forming or cytopathic effects in infected cells. To date, there have been no reports of VSV pseudotyped with the S protein of a coronavirus. Pseudotyping of SARS-CoV-S protein using the VSVΔG* system may have advantages for studying the functions of SARS-CoV-S protein, as well as for developing a rapid detection system to examine neutralizing antibodies specific for SARS-CoV infection.

To generate VSV pseudotyped with SARS-CoV-S protein, we first constructed an expression plasmid encoding full-length SARS-CoV-S protein. The cDNA of SARS-CoV-S protein was amplified using forward primer S-Bam-f (5′-GGATCCAAGTGATATTCTTGTTAACAAC-3′) and reverse primer S-Bam-r (5′-GGATCCAAGAGTAAAAAA-TCTCATAAAC-3′) and cloned into the expression vector pKS336 (Saijo *et al.*, 2002). The resulting plasmid, pKS-SARS-S, was transfected into 293T cells (see Supplementary Fig. S1, available in JGV Online), followed by infection with VSVΔG* (Matsuura *et al.*, 2001). When the culture supernatants of the infected 293T cells were inoculated on to Vero E6 cells, commonly used for SARS-CoV propagation, only small numbers of GFP-expressing cells were observed (data not shown). This result indicated that the VSV pseudotype bearing the full-length SARS-CoV-S protein was not very infectious. Next, we generated an expression plasmid encoding a C-terminal-truncated version of the SARS-CoV-S protein. The cDNA of C-terminal-truncated SARS-CoV-S protein was amplified from pKS-SARS-S using forward primer S-Bam-f and reverse primer S-Bam19r (5′-GGG-ATCCTTAGCAGCAAGAACCACAAGAGCATG-3′), followed by cloning into pKS336. The resulting plasmid, pKS-SARS-St19, encoded the full-length SARS-CoV-S protein except for the C-terminal 19 aa. When 293T cells were transfected with the expression plasmid pKS-SARS-St19, expression of the S protein was detected on the cell membrane (Supplementary Fig. S1). In contrast, transfection of the plasmid pKS-SARS-St19rev, in which the cDNA of C-terminal truncated SARS-CoV-S protein was inserted in the reverse orientation, did not show expression of SARS-CoV-S protein and was therefore used as a negative control for generating the VSV pseudotype. To generate a VSV pseudotype with the C-terminal truncated SARS-CoV-St19 protein, we inoculated VSVΔG* on to 293T cells transfected with either pKS-SARS-St19 or pKS-SARS-St19rev. VSVΔG*-G was used as a positive control, in which the deleted VSV-G protein was provided *in trans* encoded by pCAG-VSV-G (a kind gift from Dr Y. Matsuura, Osaka University, Japan) (Fig. 1a). The SARS-CoV-S protein-bearing VSV pseudotype, referred to as VSV-SARS-St19, obtained from 293T cells transfected with pKS-SARS-St19, efficiently infected Vero E6 cells (Fig. 1a). The titre of VSV-SARS-St19 was $5{\cdot}0 \times 10^5$ infectious units (IU) ml^{-1}. Since partial deletion of the SARS-CoV-S protein cytoplasmic domain allowed efficient incorporation into VSV particles and led to the generation of pseudotype at high titre, it was suggested that the intact cytoplasmic domain of SARS-CoV-S protein may have interrupted correct assembly of the pseudotype particles.

In order to confirm that the SARS-CoV-St19 protein was indeed incorporated into VSV particles, VSV pseudotypes were purified by ultracentrifugation using an RPS40T rotor (Hitachi) at 35 000 r.p.m. for 1 h through 20 % sucrose and then analysed by Western blotting using a rabbit antibody specific for aa 1124–1140 of SARS-CoV-S protein (Imgenex), a rabbit anti-VSV-G antibody (a kind gift from Dr S. Nagata, Tokyo University, Japan) and a mouse monoclonal antibody specific for VSV-M (a kind gift from Dr M. A. Whitt, GTx, Inc., TN, USA) (Fig. 1b). The VSV-M and SARS-CoV-S proteins were detected in VSV-SARS-St19, whereas the VSV-M and -G protein were detected in VSVΔG*-G. These results indicated that the SARS-CoV-St19 protein expressed in 293T cells was incorporated efficiently into VSV particles.

To determine the optimal incubation period for detection of VSV-SARS-St19 infection, we performed a time-course analysis of GFP expression. Vero E6 monolayers on 24-well glass slides were infected with VSV-SARS-St19. At various time points p.i., cells were photographed under a fluorescent microscope. The number of GFP-expressing cells in the photographs was counted using ImageJ software (http://rsb.info.nih.gov/ij/). Interestingly, GFP expression was detected clearly at 7 h p.i., although the fluorescence intensity of GFP expression was increased at 9 h p.i. (Fig. 1c). Infected cells detached from culture slides, presumably due to a cytopathic effect of VSV proteins, after incubation for 16 h (data not shown). As pseudoviruses are unable to produce progeny viruses, this system would be useful for the evaluation of cell entry mechanisms mediated by SARS-CoV-S protein. Therefore, the infection efficiency of VSV-SARS-St19 can be evaluated without incubation for up to 16 h p.i. Time-course analysis of the number of GFP-positive cells showed that quantification of VSV-SARS-St19 infection was possible at 7 h p.i. (Fig. 1c). Therefore, we counted the number of GFP-positive cells infected with VSV-SARS-St19 at 7 h p.i. for further study.

To confirm the specificity of infection, a rabbit anti-SARS-CoV antibody was tested for its ability to neutralize VSV-SARS-St19. The antibody was raised against UV-inactivated, purified SARS-CoV and reacted with SARS-CoV-S protein in an immunofluorescence assay (see Supplementary Fig. S1); the antibody showed neutralizing activity against SARS-CoV infection on Vero E6 cells at a dilution of 1 : 2560 (data not shown). As a negative control, we used a rabbit antibody raised against SARS-CoV-N protein-specific oligopeptides (Mizutani *et al.*, 2004). Culture medium containing 500 IU VSV-SARS-St19 was pre-incubated with serially diluted antibodies followed by inoculation on to Vero E6 cells. Pre-incubation with anti-SARS-CoV antibody showed

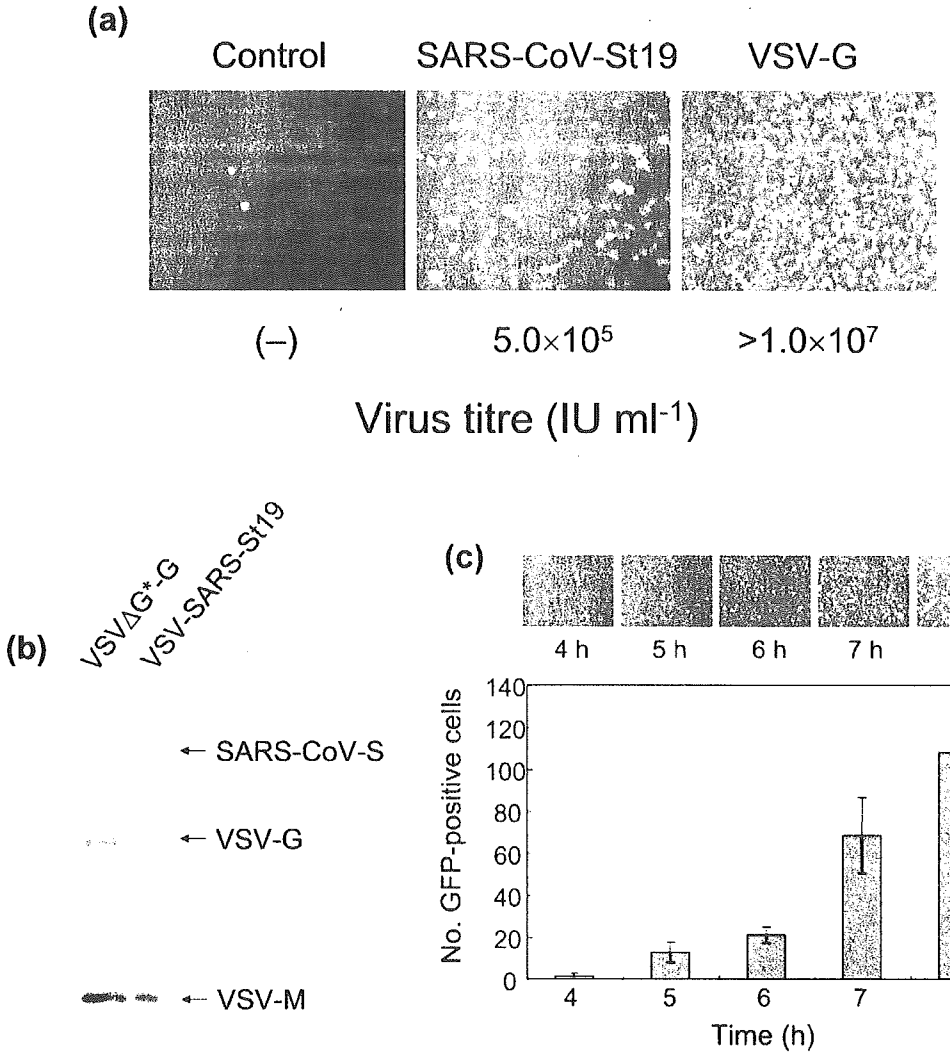

Fig. 1. Generation and characterization of VSV pseudotyped with SARS-CoV-S protein. (a) VSVΔG* was inoculated on to 293T cells expressing the indicated glycoproteins. After 24 h, culture supernatants were collected, filtered through a 0·22 μm pore size filter and inoculated on to Vero E6 cells. GFP expression was examined under a fluorescent microscope. The titre of pseudotypes viruses was determined by end-point dilution. (b) Incorporation of SARS-CoV-S protein into pseudotype VSV particles. VSV-SARS-St19 and VSVΔG*-G were partially purified by ultracentrifugation through 20% sucrose. Viral proteins were analysed by Western blotting. The bands of SARS-CoV-S protein (180 kDa), VSV-G protein (62 kDa) and VSV-M protein (32 kDa) are indicated. (c) Rapid detection and quantification of VSV-SARS-St19 infection. Vero E6 cells were infected with VSV-SARS-St19 and GFP expression was examined at the indicated time points p.i. under a fluorescent microscope. The bar graph represents the number of GFP-positive cells per microscopic field (mean ± SD) calculated from six fields.

a significant reduction in the titre of VSV-SARS-St19 in a dose-dependent manner (Fig. 2a). Fifty per cent neutralizing activity was calculated at a dilution of 1 : 2000. In contrast, infection of Vero E6 cells with VSVΔG*-G was not affected by the anti-SARS-CoV antibody, even at a lower dilution (1 : 80 dilution) (Fig. 2a). When VSV-SARS-St19 was pre-incubated with control anti-SARS-CoV-N antibody, no neutralizing activity was observed (Fig. 2a). The possibility of carry-over of VSV-G during the production of VSV-SARS-St19, leading to infection of Vero E6 cells, was excluded, since an anti-VSV-G monoclonal antibody (P2F3, a kind gift from Dr. S. Nagata), which showed specific neutralizing activity against VSV infection (Nagata *et al.*, 1992), had no effect on infection of Vero E6 cells by VSV-SARS-St19 (Fig. 2b), but prohibited infection by VSVΔG*-G. These results indicated that infection of Vero E6 cells with

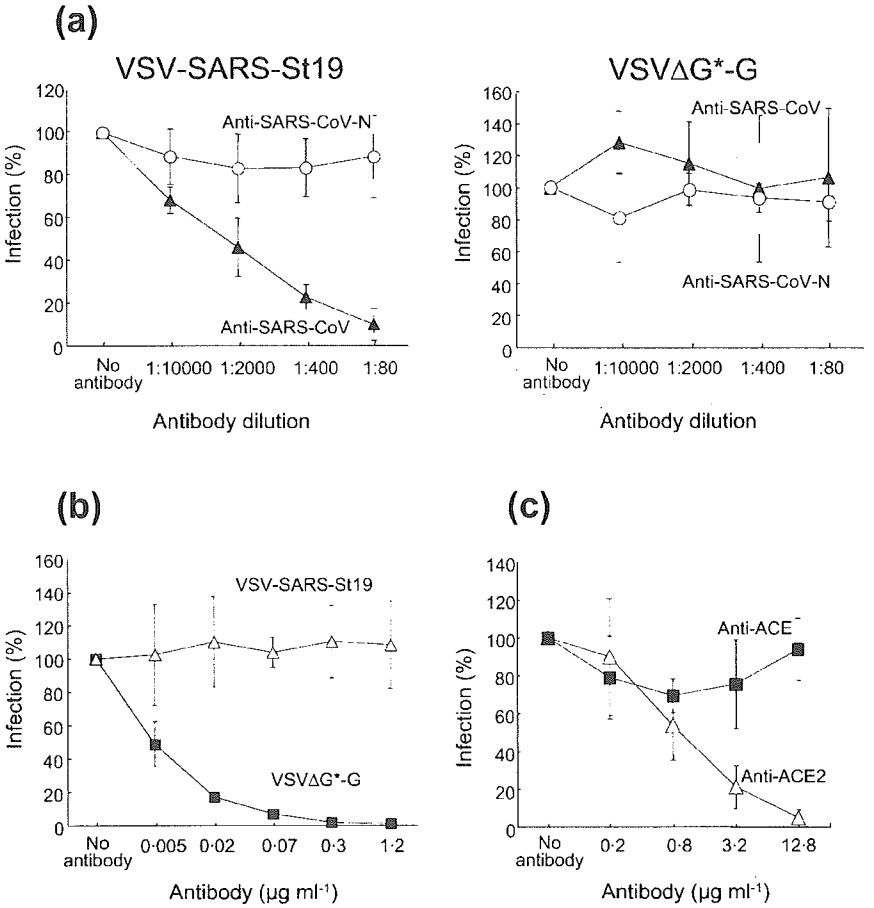

Fig. 2. Specificity of VSV-SARS-St19 pseudotype infection. (a) VSV-SARS-St19 (left) or VSVΔG*-G (right) was pre-incubated with serially diluted anti-SARS-CoV (▲) or anti-SARS-CoV-N (○) followed by inoculation on to Vero E6 cells. (b) VSV-SARS-St19 (△) or VSVΔG*-G (■) was pre-incubated with serially diluted anti-VSV-G antibody. (c) Vero E6 cells were pre-incubated with serially diluted anti-ACE (■) or anti-ACE2 (△) antibody and infected with VSV-SARS-St19. At 7 h p.i., GFP-positive cells were counted. The number of GFP-positive cells in the absence of antibodies was set as 100 %. The results are shown as mean ± SD for at least three independent assays.

VSV-SARS-St19 was mediated solely by SARS-CoV-S protein.

To determine whether anti-ACE2 antibody could inhibit VSV-SARS-St19 infection, Vero E6 cells were pre-incubated with anti-ACE2 antibody (R&D Systems) and the infectivity of VSV-SARS-St19 was examined. As a negative control, cells were pre-incubated with anti-ACE antibody (R&D Systems). As shown in Fig. 2(c), pre-incubation with anti-ACE2 antibody resulted in a significant reduction in VSV-SARS-St19 infection in a dose-dependent manner. Anti-ACE2 antibody, at a concentration of 12·8 μg ml^{-1}, completely inhibited VSV-SARS-St19 infection. In contrast, anti-ACE antibody had no appreciable effect on infection. These results indicated that VSV-SARS-St19 infection is ACE2-dependent. These observations were consistent with those reported previously by Li *et al.* (2003); on SARS-CoV infection of Vero E6 cells, the same polyclonal antibody showed an inhibitory effect on cytopathicity in a dose-dependent manner and complete inhibition was observed at an anti-ACE2 antibody concentration of approximately 10 μg ml^{-1}.

We further analysed whether soluble ACE2 protein could inhibit infection by VSV-SARS-St19. We introduced two amino acid substitutions at aa 374 and 378 within the putative catalytic domain of ACE2 (soACE2-NN; Supplementary Fig. S2). Purified soACE2-NN protein expressed in a baculovirus expression system was pre-incubated with VSV-SARS-St19 or VSVΔG*-G and the mixtures inoculated on to Vero E6 cells. As shown in Fig. 3(a), soluble ACE2 protein strongly inhibited VSV-SARS-St19 infection in a dose-dependent manner, but did not affect VSVΔG*-G infection. These observations indicated that purified soluble ACE2 specifically inhibited VSV-SARS-St19 infection. The highest concentration of soACE2 showed partial inhibition

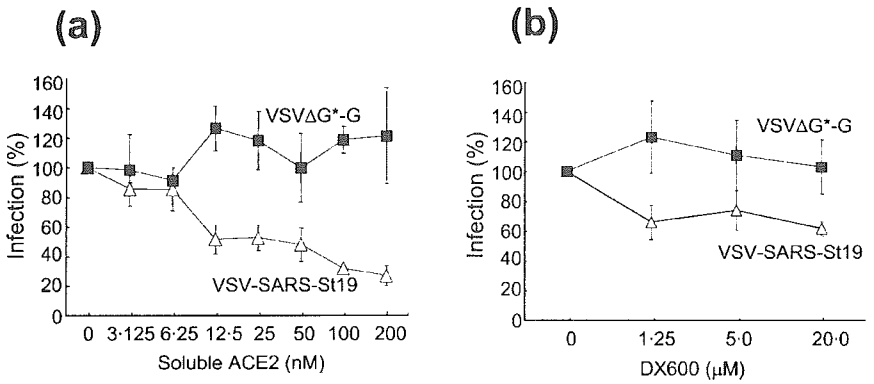

Fig. 3. Inhibition of VSV-SARS-St19 infection. VSV-SARS-St19 (△) or VSVΔG*-G (■) was pre-incubated with serially diluted soACE2NN (a) or DX600 (b), followed by inoculation on to Vero E6 cells. The infectivity of the pseudotypes was examined as described in Fig. 2.

(70–80 %) of VSV-SARS-St19 infectivity. However, the possibility that ACE2-independent entry of the pseudotype virus also existed could be excluded, since anti-ACE2 antibody completely inhibited VSV-SARS-St19 infectivity and almost all of the infection was dependent on ACE2 (Fig. 2c). The amount of soluble ACE2 that neutralized 50 % of the VSV-SARS-St19 infection (50 % neutralizing dose; ND_{50}) was estimated to be 12·5 nM. The neutralization activity of soACE2 in the present study was somewhat lower than that reported by Moore *et al.* (2004). This may have been due to the different strategies used for soACE2 preparation. The neutralization activity of soACE2 against SARS-CoV infection was lower than that of soluble mouse hepatitis virus receptor (soMHVR) against MHV infection (ND_{50} = 1 nM; Miura *et al.*, 2004; Zelus *et al.*, 1998). These observations suggested that SARS-CoV infection is regulated less strictly by the receptor function than MHV infection. Alternatively, a subdomain of ACE2 protein might represent increasing neutralization activity if bound to the SARS-CoV-S protein more strongly than the full-length protein. Indeed, neutralization of MHV-A59 infection was enhanced when the N-terminal subdomain of MHVR was used for neutralization experiments (Zelus *et al.*, 1998). It is noteworthy that an alternative splice variant of mouse ACE2 mRNA, consisting of the 5′ half of mouse ACE2 mRNA and not containing the metalloproteinase catalytic domain, has been reported (Komatsu *et al.*, 2002).

We then investigated whether a known ACE2-specific peptide inhibitor competed against ACE2-mediated pseudotype virus infection. VSV-SARS-St19 was pre-incubated with various concentrations of DX600 (Phoenix Pharmaceuticals), which has been shown to bind to and inhibit the enzymic activity of ACE2 (Huang *et al.*, 2003), and the mixture was then inoculated on to Vero E6 cells. Interestingly, DX600 inhibited VSV-SARS-St19 infection, but did not inhibit VSVΔG*-G infection. Higher concentrations (>1·25 μM) of DX600 were required for 30–40 % inhibition, indicating that this inhibition was weak (Fig. 3b). It has been shown that enzymic activity is not required for ACE2 protein as a SARS-CoV receptor (Li *et al.*, 2003). However, our results indicated that incubation of DX600 partially influenced the ACE2 function as a SARS-CoV receptor. Further investigation including inhibition studies with live SARS-CoV will be needed to elucidate the efficacy of DX600. Our results suggest that ACE2-binding peptides can be used as specific inhibitors of SARS-CoV-S protein-mediated infection. Based on the results of neutralization experiments using anti-SARS-CoV antibody and anti-ACE2 antibody, we conclude that VSV-SARS-St19 infection of target cells is mediated by SARS-CoV-S protein. The assay system described here would be useful not only for developing a safe and rapid method of detecting neutralizing antibodies to SARS-CoV, but also for screening of inhibitors of SARS-CoV-S protein-mediated infection.

Acknowledgements

We thank Dr M. A. Whitt for providing the VSVΔG* and anti-VSV-M antibody, Dr S. Nagata for providing monoclonal antibody P2F3 and rabbit anti-VSV G antibody, and Dr Y. Matsuura for providing pCAG-VSVG. We also thank Ms M. Ogata for her assistance. This work was supported in part by a grant-in-aid from the Ministry of Health, Labor and Welfare of Japan and the Japan Health Science Foundation, Tokyo, Japan.

References

Drosten, C., Gunther, S., Preiser, W. & 23 other authors (2003). Identification of a novel coronavirus in patients with severe acute respiratory syndrome. *N Engl J Med* **348**, 1967–1976.

Fouchier, R. A., Kuiken, T., Schutten, M. & 7 other authors (2003). Aetiology: Koch's postulates fulfilled for SARS virus. *Nature* **423**, 240.

Giroglou, T., Cinatl, J., Jr, Rabenau, H., Drosten, C., Schwalbe, H., Doerr, H. W. & von Laer, D. (2004). Retroviral vectors pseudotyped with severe acute respiratory syndrome coronavirus S protein. *J Virol* **78**, 9007–9015.

Hofmann, H., Geier, M., Marzi, A., Krumbiegel, M., Peipp, M., Fey, G. H., Gramberg, T. & Pohlmann, S. (2004). Susceptibility to SARS coronavirus S protein-driven infection correlates with expression of angiotensin converting enzyme 2 and infection can be blocked by soluble receptor. *Biochem Biophys Res Commun* **319**, 1216–1221.

Huang, L., Sexton, D. J., Skogerson, K. & 13 other authors (2003). Novel peptide inhibitors of angiotensin-converting enzyme 2. *J Biol Chem* **278**, 15532–15540.

Komatsu, T., Suzuki, Y., Imai, J., Sugano, S., Hida, M., Tanigami, A., Muroi, S., Yamada, Y. & Hanaoka, K. (2002). Molecular cloning, mRNA expression and chromosomal localization of mouse angiotensin-converting enzyme-related carboxypeptidase (mACE2). *DNA Seq* **13**, 217–220.

Ksiazek, T. G., Erdman, D., Goldsmith, C. S. & 23 other authors (2003). A novel coronavirus associated with severe acute respiratory syndrome. *N Engl J Med* **348**, 1953–1966.

Li, W., Moore, M. J., Vasilieva, N. & 9 other authors (2003). Angiotensin-converting enzyme 2 is a functional receptor for the SARS coronavirus. *Nature* **426**, 450–454.

Marra, M. A., Jones, S. J., Astell, C. R. & 56 other authors (2003). The genome sequence of the SARS-associated coronavirus. *Science* **300**, 1399–1404.

Matsuura, Y., Tani, H., Suzuki, K. & 8 other authors (2001). Characterization of pseudotype VSV possessing HCV envelope proteins. *Virology* **286**, 263–275.

Miura, H. S., Nakagaki, K. & Taguchi, F. (2004). N-terminal domain of the murine coronavirus receptor CEACAM1 is responsible for fusogenic activation and conformational changes of the spike protein. *J Virol* **78**, 216–223.

Mizutani, T., Fukushi, S., Saijo, M., Kurane, I. & Morikawa, S. (2004). Phosphorylation of p38 MAPK and its downstream targets in SARS coronavirus-infected cells. *Biochem Biophys Res Commun* **319**, 1228–1234.

Moore, M. J., Dorfman, T., Li, W. & 9 other authors (2004). Retroviruses pseudotyped with the severe acute respiratory syndrome coronavirus spike protein efficiently infect cells expressing angiotensin-converting enzyme 2. *J Virol* **78**, 10628–10635.

Nagata, S., Okamoto, Y., Inoue, T., Ueno, Y., Kurata, T. & Chiba, J. (1992). Identification of epitopes associated with different biological activities on the glycoprotein of vesicular stomatitis virus by use of monoclonal antibodies. *Arch Virol* **127**, 153–168.

Nie, Y., Wang, P., Shi, X. & 13 other authors (2004). Highly infectious SARS-CoV pseudotyped virus reveals the cell tropism and its correlation with receptor expression. *Biochem Biophys Res Commun* **321**, 994–1000.

Ogino, M., Ebihara, H., Lee, B. H., Araki, K., Lundkvist, A., Kawaoka, Y., Yoshimatsu, K. & Arikawa, J. (2003). Use of vesicular stomatitis virus pseudotypes bearing Hantaan or Seoul virus envelope proteins in a rapid and safe neutralization test. *Clin Diagn Lab Immunol* **10**, 154–160.

Rota, P. A., Oberste, M. S., Monroe, S. S. & 32 other authors (2003). Characterization of a novel coronavirus associated with severe acute respiratory syndrome. *Science* **300**, 1394–1399.

Saijo, M., Qing, T., Niikura, M., Maeda, A., Ikegami, T., Sakai, K., Prehaud, C., Kurane, I. & Morikawa, S. (2002). Immunofluorescence technique using HeLa cells expressing recombinant nucleoprotein for detection of immunoglobulin G antibodies to Crimean-Congo hemorrhagic fever virus. *J Clin Microbiol* **40**, 372–375.

Simmons, G., Reeves, J. D., Rennekamp, A. J., Amberg, S. M., Piefer, A. J. & Bates, P. (2004). Characterization of severe acute respiratory syndrome-associated coronavirus (SARS-CoV) spike glycoprotein-mediated viral entry. *Proc Natl Acad Sci U S A* **101**, 4240–4245.

Takada, A., Robison, C., Goto, H., Sanchez, A., Murti, K. G., Whitt, M. A. & Kawaoka, Y. (1997). A system for functional analysis of Ebola virus glycoprotein. *Proc Natl Acad Sci U S A* **94**, 14764–14769.

Tatsuo, H., Okuma, K., Tanaka, K., Ono, N., Minagawa, H., Takade, A., Matsuura, Y. & Yanagi, Y. (2000). Virus entry is a major determinant of cell tropism of Edmonston and wild-type strains of measles virus as revealed by vesicular stomatitis virus pseudotypes bearing their envelope proteins. *J Virol* **74**, 4139–4145.

Zelus, B. D., Wessner, D. R., Williams, R. K., Pensiero, M. N., Phibbs, F. T., deSouza, M., Dveksler, G. S. & Holmes, K. V. (1998). Purified, soluble recombinant mouse hepatitis virus receptor, $Bgp1^b$, and Bgp2 murine coronavirus receptors differ in mouse hepatitis virus binding and neutralizing activities. *J Virol* **72**, 7237–7244.

Journal of Medical Virology 77:83–88 (2005)

Antigen-Capture Enzyme-Linked Immunosorbent Assay for the Diagnosis of Crimean-Congo Hemorrhagic Fever Using a Novel Monoclonal Antibody

Masayuki Saijo,[1]* Qing Tang,[2] Bawudong Shimayi,[3] Lei Han,[2] Yuzhen Zhang,[4] Muer Asiguma,[4] Dong Tianshu,[4] Akihiko Maeda,[1] Ichiro Kurane,[1] and Shigeru Morikawa[1]

[1]*Special Pathogens Laboratory, Department of Virology 1, National Institute of Infectious Diseases, 4-7-1 Gakuen, Musashimurayama, Tokyo, Japan*
[2]*Second Division of Viral Hemorrhagic Fever, Institute of Infectious Disease Control and Prevention, Chinese Center for Disease Control and Prevention, P.O. Box 5, Beijing, P.R. China*
[3]*Bachu County Center for Disease Prevention and Control, Kashi District, the Xinjiang Autonomous Region, P.R. China*
[4]*Bachu People's Hospital, Bachu County, Kashi district, the Xinjiang Uygur Autonomous Region, P.R. China*

An antigen-capture enzyme-linked immunosorbent assay (ELISA) was developed for the diagnosis of Crimean-Congo hemorrhagic fever (CCHF) using a novel monoclonal antibody, 1B7, to the recombinant nucleoprotein (rNP) of CCHF virus (CCHFV) Chinese strain 8402. This ELISA detected at least 2 ng/100 μl of CCHFV rNP of 8402 and of the Nigeria strain Ibr 10200, and also detected authentic nucleoproteins (NP) of Chinese strains. Although the sensitivity of the ELISA was lower than that of nested reverse transcription polymerase chain reaction (RT-PCR), it was able to detect nucleoproteins in acute sera of CCHF patients. The presence of anti-CCHFV IgG decreased the sensitivity of the ELISA, possibly due to competition with 1B7, and this would tend to limit application of the ELISA. However, the method may be useful for the diagnosis of CCHF patients in the acute stage of illness, especially in laboratories not equipped with RT-PCR testing capabilities. ***J. Med. Virol. 77:83–88, 2005.***

KEY WORDS: Crimean-Congo hemorrhagic fever; diagnosis; nucleoprotein; monoclonal antibody; ELISA

INTRODUCTION

Crimean-Congo hemorrhagic fever (CCHF) virus (CCHFV) is a member of the family Bunyaviridae, genus *Nairovirus* [Nichol, 2001]. Humans acquire infection primarily through tick (genus *Hyalomma*) bites or contact with fresh meat or blood from slaughtered viremic animals, including sheep, cattle, and goats [Nichol, 2001]. CCHFV infections have been reported in Africa, Eastern Europe, the Middle East, and Central and Southern Asia, although human cases are believed to be underreported because disease usually occurs in remote areas. Nosocomial outbreaks of CCHF have also been reported [Burney et al., 1980; Suleiman et al., 1980; Joubert et al., 1985; van de Wal et al., 1985; Fisher-Hoch et al., 1995; Papa et al., 2002, 2004].

Ribavirin has been shown to inhibit replication of CCHFV in vitro and in vivo [Watts et al., 1989; Tignor and Hanham, 1993]. Although controlled clinical trials have not been conducted, several groups have reported successful treatment of CCHF patients with ribavirin [van de Wal et al., 1985; Fisher-Hoch et al., 1995; Papa et al., 2002, 2004; Tang et al., 2003]. Therefore, rapid diagnosis of CCHF may result in early and effective treatment, as well as subsequent prevention of nosocomial infection.

A CCHFV recombinant nucleoprotein (rNP)-based enzyme-linked immunosorbent assay (ELISA) and immunofluorescent assay for detecting immunoglobulin (Ig) G antibodies to CCHFV were described previously [Saijo et al., 2002a,b]. Detection of CCHFV IgM antibodies is another reliable procedure for rapid diagnosis of CCHF [Tang et al., 2003; Saijo et al., 2005]. However, CCHFV-antigen detection is considered to be more

Grant sponsor: The Ministry of Health, Labor and Welfare of Japan.

*Correspondence to: Dr. Masayuki Saijo, Special Pathogens Laboratory, Department of Virology 1, National Institute of Infectious Diseases, 4-7-1 Gakuen, Musashimurayama, Tokyo 208-0011, Japan. E-mail: msaijo@nih.go.jp

Accepted 4 May 2005
DOI 10.1002/jmv.20417
Published online in Wiley InterScience (www.interscience.wiley.com)

useful for rapid diagnosis of CCHF. In the past, CCHFV-antigen detection ELISA system was developed and used for diagnosis of CCHF [Logan et al., 1993; Khan et al., 1997]. Sheep antibody to CCHFV was used as a capture-antibody and mouse hyperimmune ascitic fluid against CCHFV was used as a detector-antibody in the system previously reported [Logan et al., 1993]. In the present study, a novel monoclonal antibody to the rNP of CCHFV Chinese strain 8402 was produced and characterized. An antigen-capture ELISA system using this monoclonal antibody was subsequently developed, and its use in the diagnosis of CCHF was compared with that of nested reverse transcription polymerase chain reaction (RT-PCR).

MATERIALS AND METHODS

Cell Culture

Hybridomas and their parental cell line, P3/Ag568, plus high five (Tn5) insect cells, were cultured as previously described [Niikura et al., 2001].

Recombinant Baculoviruses

Recombinant baculoviruses expressing 6X histidine-tagged rNP of CCHFV Chinese strain 8402 and Nigerian strain Ibr 10200 were used as described previously [Saijo et al., 2002a].

Authentic CCHFVs

Six CCHFV Chinese strains (66019, 7001, 7803, 78024, 88166, and 8402) were used. Viral antigens were prepared from newborn mouse brains inoculated with each of the virus strains. Antigens were inactivated by treatment with detergent, 1% Triton-X in phosphate buffered saline solution (PBS), and ultraviolet irradiation for more than 1 hr.

rNP of CCHFV

The full-length rNP of CCHFV, consisting of 482 amino acid residues, was expressed using a baculovirus system [Saijo et al., 2002a]. rNP was purified by utilizing the Ni^{2+}-resin purification system (Qiangen GmbH, Hilden, Germany). Protein concentrations of purified rNP were measured by the Bradford method using Protein Assay™ according to the manufacturer's instructions (Bio-Rad Laboratories, Hercules, CA).

Establishment of Monoclonal Antibodies

Monoclonal antibodies were generated as previously described except for the immunizing antigen [Niikura et al., 2001]; BALB/c mice were immunized with purified His-CCHFV rNP in the present study.

Polyclonal Antibodies

Polyclonal antibodies were induced in rabbits and in monkeys (*Macaca fascicularis*) by immunization with the purified rNP of CCHFV Chinese strain 8402 expressed in the baculovirus system [Saijo et al., 2002a]. Mouse hyperimmune ascites fluid (MHAF) against CCHFV (courtesy of T.G. Ksiazek), along with monoclonal antibodies to glutathione-*S*-transferase (GST) produced in our laboratory, were also used.

Antigen-Capture ELISA

Antigen-capture ELISA was performed as described previously [Niikura et al., 2001]. In this study, each of the purified monoclonal antibodies to CCHFV rNP were coated on 96-microwell immunoplates (Falcon, Becton Dickinson Labware, Franklin Lakes, NJ). For detection of antigen, each of the purified monoclonal antibodies was diluted in PBS solution and 100 μl adsorbed overnight at 4°C on to the immunoplates. Control wells were similarly adsorbed with PBS. The capture and control wells were washed three times with PBS supplemented with 0.05% tween-20 (PBS-T). Serum samples, positive antigen or negative antigens were diluted with 5% skimmed milk in PBS-T (M-PBS-T) and tested in twofold dilutions. The first of 6 wells coated with capture-antibody received 200 μl of samples diluted 1:4 or 1:8 in M-PBS-T and the other 5 wells 100 μl of M-PBS-T. Subsequently, 100 μl of material was diluted from the first well through the ensuing 5 wells. The same antigens were diluted similarly in 6 wells coated without capture-antibody in PBS. CCHFV rNP and negative control antigen were treated as above and used as positive and negative controls for each assay, respectively. Immunoplates were then incubated in a humidified condition for 1 hr at 37°C, washed three times with PBS-T, and rabbit anti-CCHFV rNP antibody was added in M-PBS-T at a dilution of 1:1,000 to all wells (100 μl/well). A further 1 hr incubation at 37°C was followed by three washes with PBS-T. One-hundred of goat anti-rabbit IgG antibody conjugated with horseradish peroxidase (Zymed) diluted 1:1,000 in M-PBS-T was added to each well, and incubated for 1 hr at 37°C. After three additional washes, 100 μl of [2,2'-azinobis(3-ethylbenzthiazolinesulfonic acid)] substrate (ABTS, Roche Diagnostics, Mannheim, Germany) was added to all wells, incubated for 30 min at room temperature, and the optical density (OD) read at 405 nm with reference read at 490 nm (OD_{405}) was obtained. The OD_{405} values of wells coated with the capture-monoclonal antibody were adjusted by subtracting the OD_{405} value for the corresponding well that had been coated without capture antibody. This adjusted OD_{405} was taken as a measure of the amount of antigen specifically bound.

Western Blotting

Monoclonal antibodies to rNP of CCHFV Chinese strain 8402 and polyclonal antibodies to CCHFV, were tested for reactivity to recombinant rNP fragments by Western blotting as previously described [Saijo et al., 2002a].

Clinical Specimens

Eleven serum samples were collected from nine suspected CCHF patients from the Xinjiang Uygur

Autonomous Region during an outbreak of the disease in 2001. Three samples were obtained from one patient on days 1, 5, and 9 of illness. The clinical course and virologic data of this patient were reported previously [Tang et al., 2003]. A single sample was collected from the eight remaining patients. Twenty-one serum samples were also collected from 12 suspected CCHF patients from the same region in 2002. Blood was collected twice (acute phase and 7 days later) in nine of the patients and once in the other three patients.

Informed Consent

All serum samples were collected from patients under informed consent. Consent from unconscious patients and children less than 20 years of age was obtained from family members.

Nested Reverse Transcription Polymerase Chain Reaction (RT-PCR)

Nested RT-PCR was performed as previously described [Rodriguez et al., 1997; Burt et al., 1998; Tang et al., 2003].

Detection of CCHFV IgG and IgM Antibodies by rNP-Based ELISA

Antibodies to CCHFV were detected by CCHFV rNP-based IgG ELISA and IgM-capture ELISA as described previously [Saijo et al., 2002a, 2005; Tang et al., 2003].

RESULTS

Generation of Monoclonal Antibodies to CCHFV rNP

Ten hybridomas clones that secrete monoclonal antibodies to CCHFV rNP were generated. All antibodies had subclass G1 and kappa-type light chains. Of the 10 clones, eight reacted strongly with CCHFV rNP by antigen-capture ELISA, approximately 8 ng/ml of CCHFV rNP was detected using each of the eight monoclonal antibodies (Fig. 1A). Antigen-capture ELISA using each of these eight monoclonal antibodies resulted in similar reactivity in detecting CCHFV rNP (Fig. 1B). However, monoclonal antibodies of clones 1E10, 1F1, 2C4, 2E10, and 1B7 reacted more strongly to authentic viral NP of CCHFV strain 66019 than those of clones 1B8, 1E5, and 3B6 (Fig. 1C). Furthermore, antigen-capture ELISA using each of the five monoclonal antibodies (1E10, 1F1, 2C4, 1B7, 2E10) detected authentic viral NPs of all five CCHFV Chinese strains (7001, 7803, 78024, 88166, 8402) tested with similar reactivity patterns (data not shown).

Detection of CCHF Antigen in Human Serum Samples

Based on the above results, monoclonal antibody clone 1B7 was selected as a capture-antibody in the antigen-capture ELISA. Human serum samples collected from three CCHF cases in acute phase during the 2001 outbreak (01–2, 01–4, 01–8) showed positive reactions by nested RT-PCR (Fig. 2A). However, only sample 01–8 reacted positive by antigen-capture ELISA (Fig. 2B). Sample 01–8, collected on day 1 of illness, did not have either IgM or IgG antibodies. However, samples collected from the same patient on days 5 and 9 (01–8* and 01–8**, respectively) had both IgM and IgG antibodies [Tang et al., 2003]. Samples 01–2 and 01–4 had IgM antibodies but no IgG antibodies.

Among the samples collected in 2002, only samples 02–2 and 02–11 (acute serum from two CCHF cases) showed positive reactions by antigen-capture ELISA (Fig. 2E). CCHFV genome fragments were amplified in

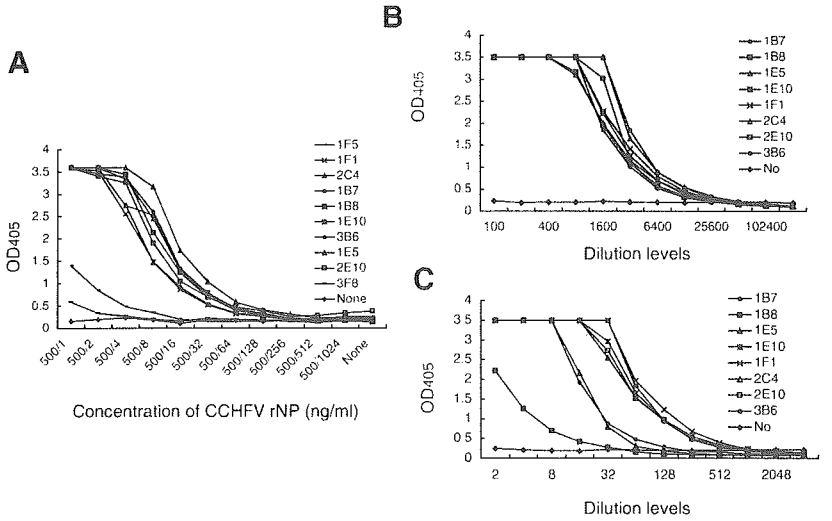

Fig. 1. Sensitivity of the antigen-capture ELISA using monoclonal antibodies in the detection of the CCHFV rNP (**A**, **B**) and the authentic nucleoprotein of CCHFV Chinese strain 66019 (**C**). Antigen-capture ELISA studies for B and C were conducted as part of the same experiment.

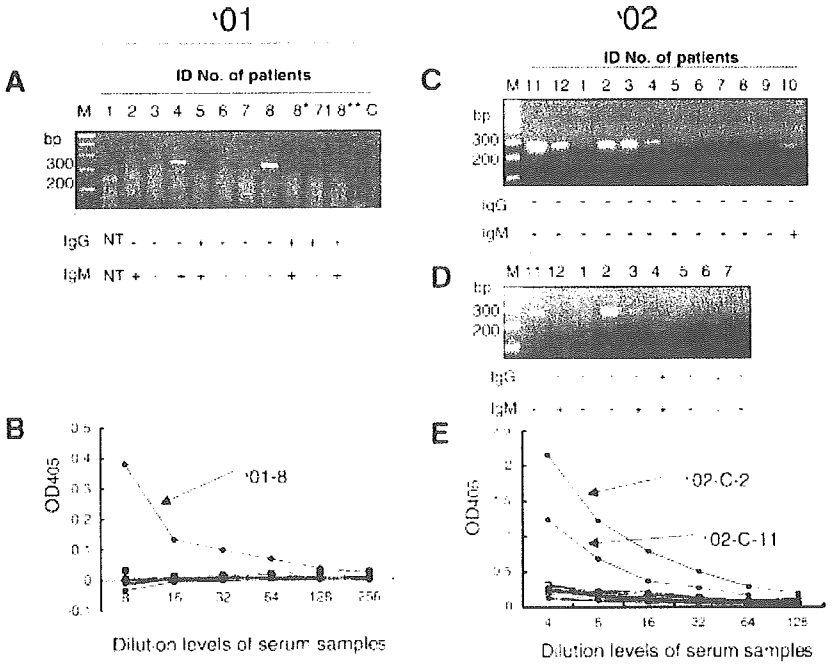

Fig. 2. Nested RT-PCR and IgG- and IgM-capture ELISA (**A**, **C**, **D**), and antigen-capture ELISA (**B**, **E**) results of serum samples collected from suspected patients with CCHF. Samples were collected from nine patients in 2001 ('01, **left panel**) and from 12 patients in 2002 ('02, **right panel**). Blood was drawn on days 1 ("8"), 5 ("8*"), and 9 ("8**") from patient No. 8. Samples in C were collected first and those in D were collected approximately 1 week after those in C. "NT" in A indicates "not tested." Samples collected in 2001 and 2002 were tested separately.

six of the 12 acute samples by nested RT-PCR (Fig. 2C). However, only 02–10 demonstrated an antibody response to CCHFV. Of the five samples (02–11, 02–12, 02–2, 02–3, 02–4) collected from patients with viremia as demonstrated by nested RT-PCR but without CCHFV antibody responses, only two samples exhibited positive reactions by antigen-capture ELISA (Fig. 2C).

Efficacy of the Antigen-Capture ELISA in Samples Containing Antibodies to CCHFV NP

The effect of the presence of anti-CCHFV antibodies on the sensitivity of the antigen-capture ELISA was investigated. CCHFV rNP diluted serially with TPBS-M solution was mixed with the monkey serum raised against CCHFV rNP (ID 3191 10Mar00) or with pre-immunized monkey serum, kept for 1 hr at room temperature, and tested for reactivity by antigen-capture ELISA. Monkey serum raised against CCHFV rNP possessed CCHFV rNP antibodies at a titer of approximately 1:6,400 (Fig. 3C). Reactivity of the ELISA decreased when antibodies to CCHFV rNP were present in the samples.

Reactivity of Monoclonal Antibody Clone 1B7 to rNP of CCHFV Strain Ibr10200

Reactivity of monoclonal antibody clone 1B7 to the rNP of CCHFV strain Ibr10200 and Chinese strain 8402 was compared by using both Western blotting and antigen-capture ELISA (Fig. 4). Both antigens reacted with monoclonal antibody 1B7 by Western blotting (Fig. 4A). Antigen-capture ELISA also detected both antigens with similar reactivity (Fig. 4B).

DISCUSSION

The antigen-capture ELISA using the monoclonal antibody 1B7 detected not only the authentic NP of CCHFV Chinese strains but also the CCHFV rNP of the Nigerian strain Ibr10200. These data suggest that other NPs of CCHFV strains besides those from Chinese strains may be detected by this ELISA.

Three of the 6 serum samples collected from patients, whose sera were RT-PCR positive and antibody-negative (01–8, 02–11, 02–12, 02–2, 02–3, and 02–4), showed positive reactions by the antigen-capture ELISA. Furthermore, 3 of 21 serum samples from suspected patients were positive by ELISA, although 9 were CCHFV genome positive by the nested RT-PCR. These data suggest that although ELISA may be useful for the diagnosis of CCHF, sensitivity is lower than nested RT-PCR.

The presence of antibodies to CCHFV NP in the samples decreased the reactivity of the antigen-capture ELISA (Fig. 3). None of the nested RT-PCR-positive and antibody-positive serum samples reacted positively by antigen-capture ELISA, suggesting that this method is useful for testing serum samples collected during the

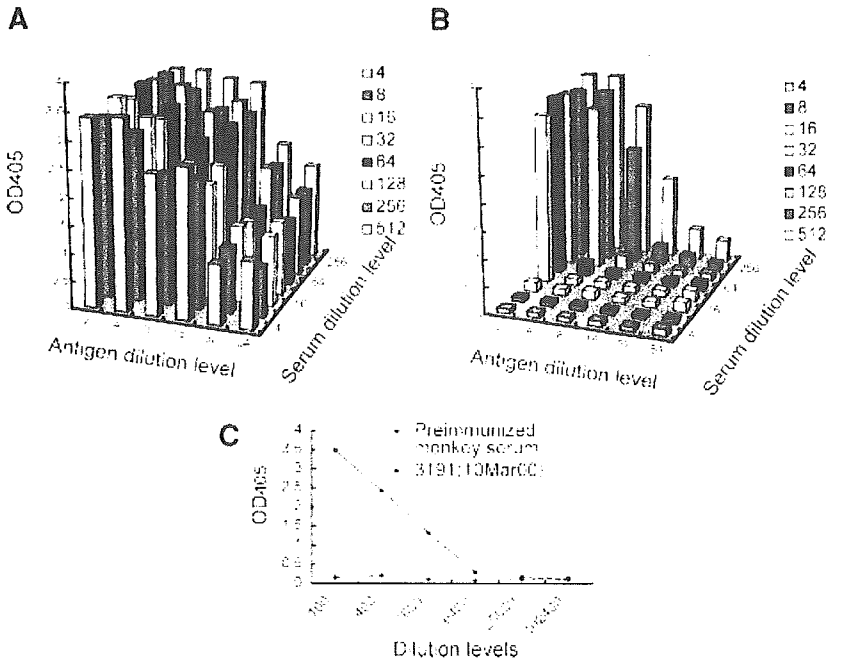

Fig. 3. Influence of CCHFV NP antibody presence toward detection of CCHFV NP by antigen-capture ELISA. CCHFV rNP mixed with monkey serum raised against CCHFV rNP were not as efficiently detected (**B**) as antigens mixed with pre-immunized monkey serum (**A**). OD_{405} values of CCHFV rNP antibody-positive and negative monkey sera are shown in figure **C**. The anti-CCHFV IgG antibody titer of sample 3191 (10Mar00) was 1:6,400, while the pre-immunized monkey serum contained no detectable antibodies (C).

acute phase of illness before antibody responses are detectable. The antigenic region is located within the CCHFV NP only in the middle section [Saijo et al., 2002a]. Monoclonal antibodies, including 1B7, recognized this region and its conformational epitopes (data not shown). It is possible that antibodies to the NP present in patients' sera inhibit the monoclonal antibodies from reacting with these epitopes. Furthermore,

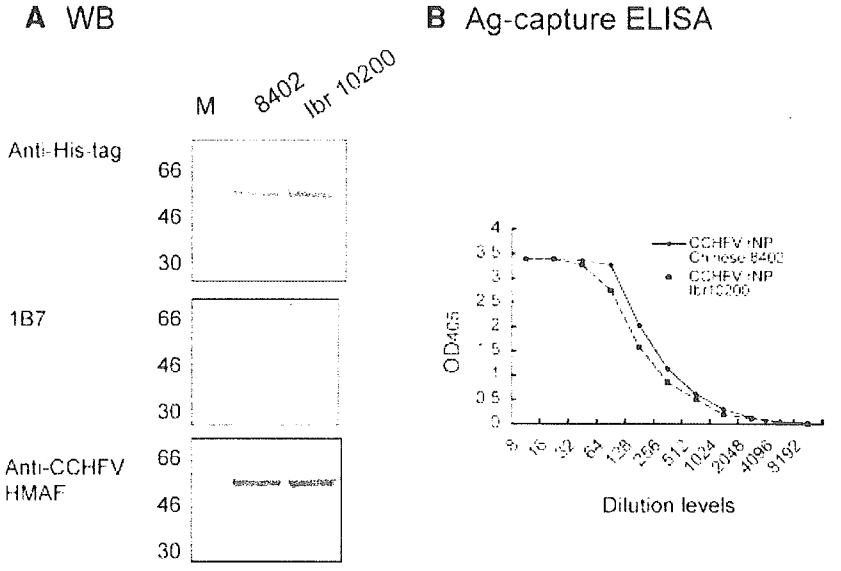

Fig. 4. Reactivity of monoclonal antibody clone 1B7 (**A, middle panel**), monoclonal antibody to His-tag (A, **upper panel**) and anti-CCHFV HMAF (A, **lower panel**) to CCHFV rNPs of CCHFV Chinese strain 8402 and CCHFV Nigerian strain Ibr10200 by Western blotting. Efficacy of the antigen-capture ELISA in detecting the CCHFV rNPs of CCHFV Chinese strain 8402 and CCHFV Nigerian strain Ibr10200 is shown in **B**. Protein concentrations of each sample were normalized in this experiment.

the amount of the CCHFV antigen decreases as time passes after illness onset. These findings may account for the low reactivity of the antigen-capture ELISA when testing antibody-positive serum samples.

The diagnostic sensitivity of the antigen-capture ELISA was verified in the present study using serum samples. However, mononuclear phagocytes are also known to be a primary target of CCHFV [Burt et al., 1997]. Therefore, it may be possible to increase the sensitivity of the ELISA by using whole blood samples instead of serum samples. Further studies are needed to address this issue.

In summary, CCHFV antigen-capture ELISA was developed using the novel monoclonal antibody clone 1B7. This ELISA was shown to be useful for the diagnosis of CCHF, especially when samples were collected during the acute phase of disease.

ACKNOWLEDGMENTS

The first and the second authors (Dr. M. Saijo, M.D., and Dr. Q. Tang, M.D.) contributed equally to this work. We thank all the staff at the Xinjiang Bachu People's Hospital, who contributed to the treatment of patients. We also thank Dr. Li Fan, Director of the AIDS Prevention and Control Center, Xinjiang Epidemic Prevention Station, Urumqi, the Xinjiang Uygur Autonomous Region, and his colleagues. We are grateful to Ms. M. Ogata, Special Pathogens Laboratory, Department of Virology 1, National Institute of Infectious Diseases, Tokyo, Japan, and Ms. X. Zhao and Ms. X. Tao, the Second Division of Viral Hemorrhagic Fever, Institute of Infectious Disease Control and Prevention, Chinese Center for Disease Control and Prevention, for their technical assistance with this project. Tests were performed in a high containment laboratory according to the regulations of the Institute of Infectious Disease Control and Prevention, Chinese Center for Disease Control and Prevention. We thank Dr. Pual Kitsutani, Infectious Disease Surveillance Center, National Institute of Infectious Diseases, Tokyo, Japan, for helpful discussion. We thank Dr. T.G. Ksiazek, Chief of the Special Pathogens Branch, Division of Viral and Rickettsial Diseases, CDC, Atlanta, GA, for providing MHAF against CCHFV and the cDNA of the S-gene of CCHFV Nigerian strain Ibr 10200. This study was approved by both the Ethical Committee on Medical Research and Human Right and the Ethical Committee on Animal Experiments, National Institute of Infectious Diseases, Tokyo, Japan.

REFERENCES

Burney MI, Ghafoor A, Saleen M, Webb PA, Casals J. 1980. Nosocomial outbreak of viral hemorrhagic fever caused by Crimean Hemorrhagic fever-Congo virus in Pakistan, January 1976. Am J Trop Med Hyg 29:941–947.

Burt FJ, Swanepoel R, Shieh WJ, Smith JF, Leman PA, Greer PW, Coffield LM, Rollin PE, Ksiazek TG, Peters CJ, Zaki SR. 1997. Immunohistochemical and in situ localization of Crimean-Congo hemorrhagic fever (CCHF) virus in human tissues and implications for CCHF pathogenesis. Arch Pathol Lab Med 121:839–846.

Burt FJ, Leman PA, Smith JF, Swanepoel R. 1998. The use of a reverse transcription-polymerase chain reaction for the detection of viral nucleic acid in the diagnosis of Crimean-Congo haemorrhagic fever. J Virol Methods 70:129–137.

Fisher-Hoch SP, Khan JA, Rehman S, Mirza S, Khurshid M, McCormick JB. 1995. Crimean Congo-haemorrhagic fever treated with oral ribavirin. Lancet 346:472–475.

Joubert JR, King JB, Rossouw DJ, Cooper R. 1985. A nosocomial outbreak of Crimean-Congo haemorrhagic fever at Tygerberg Hospital. Part III. Clinical pathology and pathogenesis. S Afr Med J 68:722–728.

Khan AS, Maupin GO, Rollin PE, Noor AM, Shurie HH, Shalabi AG, Wasef S, Haddad YM, Sadek R, Ijaz K, Peters CJ, Ksiazek TG. 1997. An outbreak of Crimean-Congo hemorrhagic fever in the United Arab Emirates, 1994–1995. Am J Trop Med Hyg 57:519–525.

Logan TM, Linthicum KJ, Moulton JR, Ksiazek TG. 1993. Antigen-capture enzyme-linked immunosorbent assay for detection and quantification of Crimean-Congo hemorrhagic fever virus in the tick, *Hyalomma truncatum*. J Virol Methods 42:33–44.

Nichol ST. 2001. Bunyaviruses. In: Knipe DM, Howley PM, editors. Fields virology. 4th edn. Philadelphia: Lippincott Williams & Wilkins. pp 1603–1633.

Niikura M, Ikegami T, Saijo M, Kurane I, Miranda ME, Morikawa S. 2001. Detection of Ebola viral antigen by enzyme-linked immunosorbent assay using a novel monoclonal antibody to nucleoprotein. J Clin Microbiol 39:3267–3271.

Papa A, Bino S, Llagami A, Brahimaj B, Papadimitriou E, Pavlidou V, Velo E, Cahani G, Hajdini M, Pilaca A, Harxhi A, Antoniadis A. 2002. Crimean-Congo hemorrhagic fever in Albania, 2001. Eur J Clin Microbiol Infect Dis 21:603–606.

Papa A, Christova I, Papadimitriou E, Antoniadis A. 2004. Crimean-Congo hemorrhagic fever in Bulgaria. Emerg Infect Dis 10:1465–1467.

Rodriguez LL, Maupin GO, Ksiazek TG, Rollin PE, Khan AS, Schwarz TF, Lofts RS, Smith JF, Noor AM, Peters CJ, Nichol ST. 1997. Molecular investigation of a multisource outbreak of Crimean-Congo hemorrhagic fever in the United Arab Emirates. Am J Trop Med Hyg 57:512–518.

Saijo M, Qing T, Niikura M, Maeda A, Ikegami T, Prehaud C, Kurane I, Morikawa S. 2002a. Recombinant nucleoprotein-based enzyme-linked immunosorbent assay for detection of immunoglobulin G antibodies to Crimean-Congo hemorrhagic fever virus. J Clin Microbiol 40:1587–1591.

Saijo M, Qing T, Niikura M, Maeda A, Ikegami T, Sakai K, Prehaud C, Kurane I, Morikawa S. 2002b. Immunofluorescence technique using HeLa cells expressing recombinant nucleoprotein for detection of immunoglobulin G antibodies to Crimean-Congo hemorrhagic fever virus. J Clin Microbiol 40:372–375.

Saijo M, Tang Q, Shimayi B, Han L, Zhang Y, Asiguma M, Tianshu D, Maeda A, Kurane I, Morikawa S. 2005. Recombinant nucleoprotein-based serological diagnosis of Crimean-Congo hemorrhagic fever virus infections. J Med Virol 75:295–299.

Suleiman MN, Muscat-Baron JM, Harries JR, Satti AG, Platt GS, Bowen ET, Simpson DI. 1980. Congo/Crimean haemorrhagic fever in Dubai. An outbreak at the Rashid Hospital. Lancet 2:939–941.

Tang Q, Saijo M, Zhang Y, Asiguma M, Tianshu D, Han L, Shimayi B, Maeda A, Kurane I, Morikawa S. 2003. A patient with Crimean-Congo hemorrhagic fever serologically diagnosed by recombinant nucleoprotein-based antibody detection systems. Clin Diagn Lab Immunol 10:489–491.

Tignor GH, Hanham CA. 1993. Ribavirin efficacy in an in vivo model of Crimean-Congo hemorrhagic fever virus (CCHF) infection. Antiviral Res 22:309–325.

van de Wal BW, Joubert JR, van Eeden PJ, King JB. 1985. A nosocomial outbreak of Crimean-Congo haemorrhagic fever at Tygerberg Hospital. Part IV. Preventive and prophylactic measures. S Afr Med J 68:729–732.

Watts DM, Ussery MA, Nash D, Peters CJ. 1989. Inhibition of Crimean-Congo hemorrhagic fever viral infectivity yields in vitro by ribavirin. Am J Trop Med Hyg 41:581–585.